Title
Surface Crystallography by Low-Energy Electron Diffraction

Authors
Somorjai, Gabor A.
Hove, M.A. Van

Publication Date
1990-04-01

LBL-27397

Center for Advanced Materials

CAM

To be published as a chapter in **Investigation of Interfaces and Surfaces**, B.W. Rossiter, J.F. Hamilton, and R.C. Baetzold, Eds., Interscience Publishers, Rochester, NY, 1990

Surface Crystallography by Low-Energy Electron Diffraction

G.A. Somorjai and M.A. Van Hove

April 1990

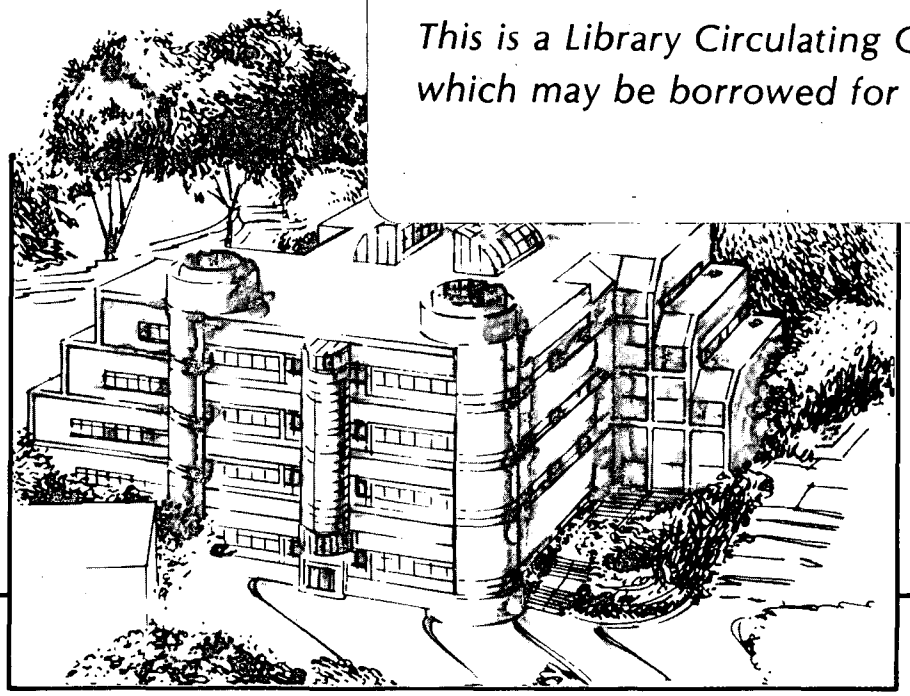

Materials and Chemical Sciences Division

Lawrence Berkeley Laboratory • University of California

ONE CYCLOTRON ROAD, BERKELEY, CA 94720 • (415) 486-4755

Prepared for the U.S. Department of Energy under Contract DE-AC03-76SF00098

DISCLAIMER

LBL-27397

SURFACE CRYSTALLOGRAPHY BY LOW-ENERGY ELECTRON DIFFRACTION

by: G.A. Somorjai and M.A. Van Hove

Center for Advanced Materials,
Materials and Chemical Sciences
Lawrence Berkeley Laboratory
1 Cyclotron Road
Berkeley, California 94720, U.S.A.
and
Department of Chemistry
University of California
Berkeley, California 94720, U.S.A.

April 1990

This work was supported in part by the Director, Office of Energy Research, Office of Basic Energy Sciences, Materials Sciences Division of the U.S. Department of Energy under Contract No. DE-AC03-76SF00098. Supercomputer time was also made available by the Office of Energy Research of the U.S. Department of Energy. A part of the theoretical development was funded by the Army Research Office.

LBL-27397

SURFACE CRYSTALLOGRAPHY BY LOW-ENERGY ELECTRON DIFFRACTION

by: G.A. Somorjai and M.A. Van Hove

Center for Advanced Materials,
Materials and Chemical Sciences
Lawrence Berkeley Laboratory
Berkeley, California 94720, U.S.A.
and
Department of Chemistry
University of California
Berkeley, California 94720, U.S.A.

Low energy electron diffraction (LEED) has become the most productive technique for surface crystallography [1-7]. The determination of bond distances and bond angles between atoms at clean solid surfaces and for atoms and molecules adsorbed on surfaces provides the molecular foundation for such diverse fields as semiconductor surface science and heterogeneous catalysis.

Several other techniques are in use for surface structure analysis, including photoelectron diffraction (PhD) [8], surface extended x-ray absorption fine structure (SEXAFS) [9,10], medium- and high-energy ion scattering (MEIS and HEIS) [11], scanning tunneling microscopy (STM) [12], and glancing angle x-ray scattering (GAXS) [13]. However, a large majority of the surface structures known at present have been solved by LEED. Nevertheless, LEED often depends on information obtained by other techniques to solve a structure [2,3]. LEED usually provides the most complete and definitive structural analysis.

In this chapter we review the experimental, theoretical, and structural advances made in the field in recent years. We first discuss the experiment. Next we familiarize the reader with the notations and nomenclature of two-dimensional surface structures and extract trends from the available data base. Then we address developments in LEED theory. The discussion that follows covers recent findings of three-dimensional LEED analysis. It starts with the structure of clean surfaces and their observed relaxations and reconstructions, as well as the structural properties of more complex clean surfaces, alloys, and compounds. Then we turn our attention to adsorbed monolayers: the surface structures of both atomic and molecular adsorbates are reviewed, including the case of coadsorption structures and disordered monolayers. In the area of

adsorbed molecular overlayers, we pay particular attention to organic molecules because of their unique importance in many fields of surface science and the rapidly expanding data base. Finally, we review the trends for crystallography by LEED for the near future.

1.1. EXPERIMENTAL ADVANCES IN LEED

In the LEED experiment [1] a well-collimated beam of electrons in the 10-300 eV range is back-scattered from the surface of a crystal. The elastically back-reflected electrons that carry the diffraction information are then separated from the inelastically scattered electrons by retarding grids and detected.

The last thirty years have seen a steady evolution in the detection of diffraction beam intensities with ever increasing signal-to-noise ratio and increasing measurement speed. In the early days the slow and cumbersome Faraday cup was used to collect the diffracted electrons. The LEED experiment benefited greatly from the development of the post-acceleration technique which utilized a fluorescent screen, from which intensities could be measured with spot photometry or by photography. This could be

carried out from behind the single crystal sample or from the back of the fluorescent screen (rear-view LEED). In recent years the video camera has become the favored detector for speed and convenience because of the ease of computer interfacing that aids data acquisition greatly. This mode of operation is called video LEED.

Developments in electron-gun designs permit one to obtain smaller diameter incident electron beams (1μm instead of 1mm) to obtain greater or variable coherence length. Lower incident electron beam currents (10^{-9} amp instead of 10^{-3} amp) are utilized in order to minimize radiation damage to the crystal or to the adsorbed monolayer. Also, surface charging can be drastically reduced in this manner on insulating surfaces. The lower diffracted intensity allows the use of modern position-sensitive detectors, instead of the fluorescent screen: resistive anodes or wedge-and-strip detectors are coupled with microchannel plates to digitally record the complete angular distribution of diffracted intensities. From such angular distributions one can generate energy-dependent beam intensities (I-V curves) or other data sets in a computer.

This type of diffraction experiment is called digital LEED (Figure 1.1). It permits the detection of diffraction beam intensities with much higher signal-to-noise ratio than video LEED [14]. As a result, it is

possible for example to measure diffuse LEED intensities, whereby intensity modulations at all collection angles can be detected to permit structure analysis from disordered monolayers.

The sample holder provides the means for rotating the crystal sample to set the desired diffraction conditions, for example normal incidence. For cleaning and temperature-dependent measurements the sample can be heated to near its melting point directly by ohmic resistance or indirectly by electron bombardment from the back. The sample can also be cooled using feedthroughs held at 77K with liquid nitrogen or to lower temperatures by the use of a liquid helium refrigerator.

The sample cleaning is carried out usually by ion bombardment using inert gas ions at low pressures ($\sim 10^{-5}$ torr) or by chemical treatments using reactive gases that are appropriate for the particular sample material. Highly reactive materials (transition metal oxides, alkali metals, etc.) rapidly become contaminated after cleaning by the diffusion of impurities from the bulk to the freshly cleaned surface or by adsorption from the gases in the ambient. In this circumstance, epitaxial layer-by-layer deposition of the material can be carried out from the vapor phase under conditions where the condensed layer atoms have enough mobility to order. For example, ordered films of iron oxide have been deposited on Pt(111) crystals by condensing a monolayer of

iron, then oxidizing it in a certain partial pressure of oxygen and finally heating so as to order it. This procedure is repeated until 10-100 ordered iron oxide layers have been deposited. In this way clean, ordered thin films of complex and reactive materials can by prepared for LEED surface crystallography studies.

1.2. TWO-DIMENSIONAL SURFACE STRUCTURES

In this section we shall be concerned with the phenomenon of two-dimensional ordering at surfaces. First the common notations will be introduced. Next we shall review the conclusions based on the experimental observation of the LEED diffraction patterns alone.

1.2.1 Notation

A LEED spot pattern represents the reciprocal lattice of the ordered surface. The diffraction pattern must be inverted to real space in order to obtain the real-space periodicity [1,5]. In this section we describe how this conversion is performed. First, the relationship between the reciprocal and real-space lattices will be given. Then the determination of the surface periodicity from the LEED pattern will be discussed.

The pattern of spots, when suitably imaged, has two-dimensional translational periodicity which can be described by the relation:

$$T^* = m^* a^* + n^* b^*, \tag{1}$$

where the two-dimensional vector T* represents a spot position, m* and n* are integers and a* and b* are the basis vectors of the reciprocal unit cell. The reciprocal lattice vectors T* are related to the real-space lattice vectors T, which we write as:

$$T = ma + nb \tag{2}$$

where m and n are integers and a and b are the basis vectors of the primitive surface unit cell. The reciprocal unit cell vectors a* and b* are related to the real-space unit-cell vectors a and b by the following equations:

$$a^* = \frac{b \times z}{a \cdot (bxz)} \tag{3a}$$

$$b^* = \frac{z \times a}{a \cdot (bxz)} \tag{3b}$$

where z is normal to the surface. The relationship between the reciprocal and real-space vectors for a two-dimensional hexagonal lattice is illustrated in Figure 1.2.

Reconstruction of the clean surface or adsorption of a gas on a surface often results in a change in the diffraction pattern corresponding to the appearance of a new surface periodicity: the new lattice is called a superlattice. This is illustrated in Figure 1.3, which shows a diffraction pattern of a clean Pt(111) surface and the diffraction pattern formed after the adsorption of an ordered layer of acetylene. Figure 1.4 shows the unit cells responsible for the diffraction patterns in Figure 1.3 superimposed on a model of the Pt(111) surface. No information concerning the location of the adsorbate species within this unit cell (the location relative to the substrate atom positions) is indicated. This information can be obtained only from analysis of the diffraction spot intensities.

To make the transition from the diffraction pattern in Figure 1.3 to the surface periodicity in Figure 1.4, we need to reference the reciprocal superlattice to the reciprocal substrate lattice defined by the vectors a* and b*. This is carried out by visual inspection of the diffraction pattern, in which the differences in spot intensities are neglected and only the positions of the diffraction beams are considered.

For the general case, the relationship of the reciprocal substrate lattice to the reciprocal superlattice is given by the equations

$$a^* = m_{11} * a^{*\prime} + m_{12} * b^{*\prime} \qquad (4a)$$

$$b^* = m_{12} * a^{*\prime} + m_{22} * b^{*\prime} \qquad (4a)$$

where a*'and b*' are the basis vectors of the reciprocal superlattice and the coefficients m_{11}^*, m_{12}^*, m_{21}^*, and m_{22}^* define the matrix

$$M^* = \begin{pmatrix} m_{11}^* & m_{12}^* \\ m_{21}^* & m_{22}^* \end{pmatrix} \tag{5}$$

In real space the superlattice is related to the substrate lattice by the equations

$$a' = m_{11} a + m_{12} b \tag{6a}$$

$$b' = m_{21} a + m_{22} b \tag{6a}$$

where a' and b' are the basis vectors of the primitive superlattice and the coefficients m_{11}, m_{12}, m_{21}, and m_{22} define the matrix

$$M = \begin{pmatrix} m_{11} & m_{12} \\ m_{21} & m_{22} \end{pmatrix} \tag{7}$$

The coefficients of the two matrices M and M* are related by the following equations:

$$m_{11} = m_{11}^* , \tag{8a}$$

$$m_{12} = m_{21}^* , \tag{8b}$$

$$m_{21} = m_{12}^* , \tag{8c}$$

$$m_{22} = m_{22}^* , \tag{8d}$$

so that if either M or M* is known, the other may be very easily obtained. In LEED experiments, M* is determined by visual inspection of the diffraction pattern and then transformed to give M, which defines the surface periodicity in real space.

A superlattice is termed commensurate when all four matrix elements m_{ij} are integers. If at least one matrix element m_{ij} is an irrational number, then the superstructure is termed incommensurate. Superlattices can be incommensurate in one surface dimension or in both surface dimensions.

Alternatively to the matrix method of denoting surface structures, another system, originally proposed by Wood [15], is more commonly used. Whereas the matrix notation can be applied to any system, Wood's notation can only be used when the angle between the superlattice vectors a' and b' is equal to the angle between the substrate vectors a and b. If this condition is met, the surface structure is labeled using the general form

$$p(u \times v)R\Phi^{o} \text{ or } c(u \times v)R\Phi^{o} \qquad (9)$$

depending on whether the unit cell is primitive or centered (the prefix p is often dropped). In Wood's notation the adsorbate unit cell is related

to the substrate unit mesh by the scale factors u and v, where

$$|a'| = u|a| \tag{10a}$$

$$|b'| = v|b| \tag{10b}$$

The label RΦ indicates a rotation of the superlattice by the angle Φ from the substrate lattice. For Φ = 0, the label RΦ is omitted. Unreconstructed surfaces of some common face-centered cubic (fcc), body-centered cubic (bcc), and hexagonal close-packed (hcp) crystal structures are shown in Figure 1.5. The unreconstructed surface has a surface unit cell that is denoted as p(1x1) or (1x1) in Wood's notation. The same surface unit lattice is denoted as $\begin{pmatrix} 1 & 0 \\ 0 & 1 \end{pmatrix}$ in the more general matrix notation. In Table 1.1 several superlattices that are commonly detected on low-Miller-index surfaces are listed with both their their Wood and matrix notations.

Table 1.1 Superlattices that are commonly observed, listed by their Wood and matrix notations.

Substrate	Superlattice unit cell	
	Wood notation	Matrix notation
fcc(100), bcc(100)	p(1×1)	$\begin{pmatrix} 1 & 0 \\ 0 & 1 \end{pmatrix}$
	c(2×2) = $(\sqrt{2} \times \sqrt{2})R45°$	$\begin{pmatrix} 1 & -1 \\ 1 & 1 \end{pmatrix}$
	p(2×1)	$\begin{pmatrix} 2 & 0 \\ 0 & 1 \end{pmatrix}$
	p(1×2)	$\begin{pmatrix} 1 & 0 \\ 0 & 2 \end{pmatrix}$
	p(2×2)	$\begin{pmatrix} 2 & 0 \\ 0 & 2 \end{pmatrix}$
	$(2\sqrt{2} \times \sqrt{2})R45°$	$\begin{pmatrix} 2 & 2 \\ -1 & 1 \end{pmatrix}$
fcc(111) (60° between basis vectors)	p(2×1)	$\begin{pmatrix} 2 & 0 \\ 0 & 1 \end{pmatrix}$
	p(2×2)	$\begin{pmatrix} 2 & 0 \\ 0 & 2 \end{pmatrix}$
	$(\sqrt{3} \times \sqrt{3})R30°$	$\begin{pmatrix} 1 & 1 \\ -1 & 2 \end{pmatrix}$
fcc(110)	p(2×1)	$\begin{pmatrix} 2 & 0 \\ 0 & 1 \end{pmatrix}$
	p(3×1)	$\begin{pmatrix} 3 & 0 \\ 0 & 1 \end{pmatrix}$
	c(2×2)	$\begin{pmatrix} 1 & -1 \\ 1 & 1 \end{pmatrix}$
bcc(110)	p(2×1)	$\begin{pmatrix} 2 & 0 \\ 0 & 1 \end{pmatrix}$

High-Miller-Index (Stepped) Surfaces

The atomic structures of high-Miller-index surfaces are composed of terraces, separated by steps, which may have kinks in them. For example, the (775) surface of an fcc crystal consists of (111) terraces, six atoms wide, separated by steps of (111) orientation and single-atom height.

The step notation [16] compacts this type of information into the general form

$$w(h_t k_t l_t) \times (h_s k_s l_s) \qquad (11)$$

where $(h_t k_t l_t)$ and $(h_s k_s l_s)$ are the Miller indices of the terrace plane and the step plane, respectively, while w is the number of atoms that are counted in the width of the terrace, including the step-edge atom and the in-step atom. Thus, the fcc(775) surface is denoted by $6(111) \times (11\bar{1})$, or also by $6(111) \times (111)$ for simplicity. A stepped surface which has steps that are themselves high-Miller-index faces is termed a kinked surface. For example, the fcc(10,8,7) = $7(111) \times (310)$ surface is a kinked surface. The step notation is, of course, equally applicable to surfaces of bcc, hcp, and other crystals, in addition to surfaces of fcc crystals. However, the overwhelming majority of experimental research on high-Miller-index surfaces so far has utilized fcc crystals.

There is another notation called "microfacet notation" [17]. This notation is based on the idea that any Miller-index vector (hkl) which specifies a certain crystal face can be decomposed in terms of three linearly independent vectors such as (111), (110), and (100). For example the fcc(10,8,7) kinked surface has the microfacet notation fcc[7_{14}(111)+1_1(110)+2_2(100)]. By using this notation, we can easily recognize that the (10,8,7) unit cell contains fourteen unit cells of the (111) microfacet, one unit cell of the (110) microfacet, and two unit cells of the (100) microfacet.

1.2.2. Review of Surface Structures Studied Through LEED Patterns

Reference [5] lists over 3,000 ordered surface structures which have been reported in the literature following observation by LEED. The low-Miller-index metal surfaces and atomic adsorbates were studied predominantly in earlier years. In recent years more emphasis has been put on the polyatomic solids (compounds, alloys) surfaces, high-Miller-index stepped surfaces and molecular overlayers with increasing complexity.

We shall in this section discuss some of the important trends that can be extracted from the observations on two-dimensional ordering listed in reference [5].

1.2.2.1 Ordering Principles

A large number of ordered surface structures can be produced experimentally. Ordering can manifest itself both as commensurate and as incommensurate structures. There are also many disordered surfaces, which often are not reported in the literature. The disordered structures are usually difficult to describe accurately and are therefore difficult to reproduce exactly in other laboratories. Nevertheless, for selected surfaces, order-order and order-disorder phase transitions have been explored in considerable detail both experimentally and theoretically. It should be stressed that many structures reported as an ordered LEED pattern may well include small or large amounts of disorder, whether in the overlayer structure or even in the substrate structure.

(i) Adsorbate-adsorbate and adsorbate-substrate interactions. The driving force for surface ordering originates, analogous to three-dimensional crystal formation, in the interactions between atoms, ions, or molecules in the surface region. The physical origin of the forces is of various types, and the spatial dependence of these interaction forces is complex.

For adsorbates, an important distinction must be made between adsorbate-substrate and adsorbate-adsorbate interactions. The dominant adsorbate-substrate interaction is due to strong covalent or ionic

chemical forces between the adsorbates and the substrate in the case of chemisorption, or to weak Van der Waals forces in the case of physisorption. Adsorbate-adsorbate interactions could be covalent bonding interactions, orbital-overlapping interactions, electrostatic interactions (e.g. dipole-dipole interactions), Van der Waals interactions, etc. These are many-body interactions that could be attractive or repulsive depending on the system.

In chemisorption it is usually the case that the adsorbate-adsorbate forces are weak compared to the adsorbate-substrate binding forces (except at very close repulsive range, since atoms will not overlap). The adsorbate-substrate interaction includes a corrugation parallel to the surface, favoring certain adsorption sites over others and implying barriers to diffusion. This imposes the constraint that only lattice sites be occupied. With weak adsorbate-adsorbate forces the locations of the adsorbed atoms or molecules are determined by the optimum adsorbate-substrate bonding.

But the adsorbate-adsorbate interactions, although usually weaker for chemisorption, still manage to dominate the long-range ordering of the overlayer. A compromise is found in the formation of an adsorbate lattice that is simply related to the substrate lattice. In the ordered case this yields commensurate superlattices. The most common of these are simple superlattices with one or two adsorbates per superlattice unit

cell. They occur for adsorbate coverages of 1/4, 1/3, 1/2, for example (we define the surface coverage to be unity when each (1x1) substrate cell is occupied by one adsorbate).

A special case of commensurate superlattice is the formation of periodic out-of-phase domains. They occur when the adsorbate coverage is not well matched to form a simple ordered lattice. Then equal domains of simple structure are mismatched to each other through dislocations (domain walls) that allow higher or lower coverages. It is not entirely straightforward to experimentally distinguish the periodic domain structures from the incommensurate structures. Therefore, many structures are found labeled as incommensurate in the literature, even though they could well be of the periodic-domain type.

An incommensurate relationship exists when there is no common periodicity between an overlayer and the substrate. This structure is dominated by adsorbate-adsorbate interactions rather than by adsorbate-substrate interactions. The classical example is that of a rare-gas monolayer physisorbed on almost any substrate: the overlayer takes on a lattice constant that is unrelated to that of the substrate. Another example of incommensurate lattice formation occurs frequently when compounds are produced by exposure of an elemental substrate to a reactive gas. Examples are metal oxides, nitrides, carbides and silicides. As soon as about one or two monolayers of the compound form on

the surface, they frequently adopt their own lattice constant independently of the unreacted substrate lattice constant. This is because the chemical bonding forces within the compound can be much stronger than those between the compound and the substrate.

(ii) Effects of adsorbate coverage. The surface coverage of an adsorbate is an important parameter in the ordering process. This is because the adsorbate-adsorbate and the adsorbate-substrate forces are strongly influenced by the distance between the adsorbates. An extreme example is alkali-metal adsorption on transition metal surfaces, where the ionicity of the adsorbate-substrate bond decreases rapidly as the surface coverage increases.

At low coverages, adsorbates may bunch together in two-dimensional islands: this occurs when there are short-range attractive adsorbate-adsorbate interactions, coupled with easy diffusion along the surface. Within each island the interactions induce an ordered arrangement of adsorbates. Other adsorbates repel each other at close adsorbate-adsorbate separations, and do not interact at the large separations: these are disordered at low coverages. But when their coverage is increased so that the mean interadsorbate distance decreases to about 3-5Å, the repulsive interactions induce and strongly influence ordering, favoring certain adsorbate configurations over others. As a result, the structure can also develop a unit cell that

repeats periodically across the surface. This is most clearly evident in the low-energy electron diffraction patterns, which depend directly on the size and orientation of this unit cell.

Most adsorbates (other than some metals) will not compress into an overlayer of unit coverage on the closest-packed metal substrates. There appears to be a close-range repulsive force that keeps them apart by approximately a Van der Waals distance (this does not necessarily imply a Van der Waals interaction, since the strongest contribution to the adsorbate-adsorbate interaction is in this case mediated by the substrate). One may attempt to compress the overlayer further by increasing the coverage, which is done by exposing the surface to the corresponding gas at high pressures. The result is either no further adsorption, or diffusion of the adsorbates into the substrate, forming compounds, or, if the temperature is low enough, formation of multilayers.

(iii) Physical adsorption. When adsorbates are used which physisorb rather than chemisorb (at suitably low temperatures), one also finds that the Van der Waals distance determines the densest overlayer packing. Here it is the Van der Waals force acting directly between the adsorbates that dominates. In this case, the optimum adsorbate-substrate bonding geometry can be overridden by the lateral adsorbate-adsorbate interactions, yielding for example incommensurate structures where the

overlayer and the substrate have independent lattices. Furthermore, with physisorption a larger coverage is also possible through multilayer formation.

(iv) Metallic adsorbates. With metallic adsorbates closer-packed overlayers can be formed. This is because metallic adsorbate atoms attract each other relatively strongly to form covalent bonds and cluster together with covalent interatomic distances. Thus at submonolayer coverages close-packed islands form. When the atomic sizes of the overlayer and substrate metals are nearly the same, one observes (1x1) structures, in which adsorbate atoms occupy every unit cell of the substrate. With less equal atomic radii, other structures are formed, dominated by the covalent closest packing distance of the adsorbate. These structures may be of the incommensurate type or, more likely, of the periodic-domain type. Beyond one close-packed overlayer, metal adsorbates frequently form multilayers or also three-dimensional crystallites. Alloy formation by interdiffusion is also observed in many cases, even in the submonolayer regime. Such surface alloys may be ordered or disordered.

1.2.2.2. Restructuring of Clean and Adsorbate Covered Surfaces

There are many observations of deviations of a clean surface structure from the structure predicted by a simple truncation of the bulk

lattice. Many LEED patterns of clean surfaces deviate from the expected (1x1) pattern; i.e., produce superlattices. These are relatively drastic cases where atoms may be displaced substantially from their bulk lattice sites and bonded to different atoms than the bulk structure would imply. Such cases are called reconstructions. Another cause of reconstruction is, as seen at compound surfaces, a change in elemental composition at a surface compared to the bulk composition. A different crystalline lattice may become favored as the surface composition changes due to segregation to or from the surface. Non-stoichiometric compounds often exhibit this behavior. A more subtle restructuring has also been discovered during full structural determinations [4,6,7]. Layer spacing relaxations have been found between the first few surface layers of the less close-packed clean metal surfaces, e.g., fcc (110) and bcc(100). These relaxations correspond to deviations of the surface bond lengths from the bulk values, but do not affect the LEED pattern.

Among the clean metal surfaces, nearly a dozen are known to reconstruct. Over 40 clean semiconductor reconstructions are reported. Numerous reconstructions have also been found for oxides and other compounds.

Some of these reconstructions and layer spacing relaxations can be explained by the tendency for bond lengths to decrease as the bonding coordination decreases. This trend fits long-established principles, as

proposed by Pauling [18], if one relates coordination number to bond order. A good illustration is presented by the reconstructions of the clean Ir, Pt and Au(100) surfaces [19]. In these three cases, the interatomic distance in the topmost layer shrinks by a few percent parallel to the surface. It then becomes more favorable for this layer to collapse into a nearly hexagonally close-packed layer rather than maintain the square lattice of the underlying layers. Many adsorbates on these surfaces can remove this reconstruction by cancelling the driving force towards smaller bond lengths.

In these studies surface cleanliness is monitored by various techniques including AES, XPS, HREELS, etc., and the sample is cleaned until the concentration of impurities is below the detection threshold of these techniques (a few hundredths of a monolayer). However, it is always risky to conclude that a reconstruction is a property of the clean surface, since it is very difficult to rule out the presence of at least some contaminants. Nevertheless, it is now believed that most of the nominally clean reconstructions are intrinsic properties of the clean surfaces, and are only marginally affected by small levels of impurities. This is the case of the Ir, Pt and Au(100) surfaces mentioned above.

At the same time it is also known that a fair number of reconstructions are adsorbate-induced [20]. Even without being ordered,

an adsorbate can induce a reconstruction, as happens with H on W(100). The clean W(100) crystal surface is itself already reconstructed, but hydrogen changes it further to another structure that varies smoothly with the hydrogen coverage. Often, the adsorbate fits periodically within the unit cell of the reconstructed substrate. This occurs, for example, with carbon on Ni(100) and sulfur on Fe(110), where the metal exhibits relatively minor, but interesting adsorbate-induced distortions.

In some cases a small coverage (below 0.1 monolayer) of disordered adsorbate can be sufficient to cause reconstruction of the substrate. This happens with alkali adatoms on Ni, Cu, Pd, and Ag(110), which transform to the missing-row structure [21-24].

Adsorbates can also restructure stepped surfaces. For example, oxygen deposited on stepped Pt surfaces has been observed to produce double-height steps. Facetting has also been observed under such circumstances.

By contrast, it is also possible, with contaminants or otherwise, to generate a metastable unreconstructed phase from a reconstructed clean surface. With suitable contaminants, such phases have been achieved with all reconstructed surfaces. In some cases, e.g., Ir(100), clean metastable structures can be obtained by appropriate heat treatments. A Si(111)-(1x1) metastable unreconstructed structure can also be achieved by laser-annealing and rapid cooling processes.

In the case of alloys, surface segregation can lead to new ordered arrangements through a change in the surface composition. In some cases, for instance CuAl(111) with a bulk composition of 16% of Al, the surface alloy orders while the bulk alloy has no long-range order [25]. One may call these alloy reordering reconstructions. They involve essentially normal lattice sites, but a different ordering at the surface compared to the bulk.

Semiconductors almost universally reconstruct when clean. This is due to the difficulty for their surface atoms to compensate for the loss of nearest neighbors, since bonding is relatively directional in semiconductors. The "dangling bonds" left by the absence of bonding partners cannot easily be used for bonding to existing surface atoms, except through more drastic rearrangements of these atoms. Therefore, most semiconductor surfaces reconstruct. Major rebonding between surface atoms occurs in this process. The associated perturbation propagates several layers into the surface until the bulk lattice is recovered. The silicon surfaces in particular have been extensively studied in their various reconstructed forms. The Si(111)-(7x7) structure is no doubt the most famous and most complex of these. Again with semiconductor surfaces, adsorbates can negate the need for reconstruction and induce a return to the bulk structure. This can happen by bonding of the adatoms to the "dangling bonds". Hydrogen does this particularly well and to some extent chemically passivates the resulting surface. More

frequently, however, adsorbates (including oxygen and metal atoms) become part of a new compound structure, by penetrating within the few topmost substrate layers.

The stoichiometry is also important in considering the reconstruction of compound semiconductors. For example a $(\sqrt{5}x\sqrt{5})R26.6^{o}$ structure of the $BaTiO_3(100)$ surface observed after high temperature annealing is considered to be due to the ordering of lattice vacancies at the surface. Similarly, the GaAs(111) surface has a (2x2) reconstruction due to Ga vacancies. Another example is the GaAs(100) surface which presents various reconstructed structures as the Ga to As ratio changes.

1.2.2.3. Simple Structures of Atomic Adsorbates at Metal Surfaces

By simple structures we mean clean unreconstructed metal surfaces with low Miller indices and atomic adsorbates thereon. These were the mainstay of the early LEED studies. In recent years this class of structures has continued to grow, mostly through new combinations of substrates and adsorbates.

The clean unreconstructed metal surfaces have, by definition, (1x1) structures. Chemisorption of non-metallic atoms causes a variety of commensurate superlattices, usually simply determined by the coverage;

e.g., c(2x2) or p(2x1) at 0.5 monolayer coverage. In the case of physisorption (e.g., for rare gas adsorption) the overlayers tend to adopt their own lattice constants, forming incommensurate overlayers.

1.2.2.4. Metallic Monolayers on Metal Crystal Surfaces

More than 400 ordered structures of metal monolayers adsorbed on metal surfaces have been reported so far [5].

At low coverages, most of the metallic adsorbates form commensurate ordered overlayers: the overlayer unit cells are closely related to the substrate unit cells. Furthermore, in many cases a (1x1) LEED pattern is observed. This suggests that adsorbed metal atoms attract each other to form 2-dimensional islands. The size of such islands can change depending on the substrate temperature, as can be detected by measuring the LEED spot size. A disordered LEED pattern is observed when the adsorbed metals repel each other. This is observed for example in the case of alkali metal adsorption on a transition metal, since the charged adatoms undergo repulsive interactions.

At higher coverages, the relative atomic sizes of the different metals becomes an important factor. When the atomic sizes of the substrate and adsorbate metals are similar, (1x1) structures are favored, whereas coincidence structures often form when the atomic sizes are much

different. As the overlayer coverage increases towards saturation of a monolayer, the adsorbate-adsorbate interaction increases. Then an incommensurate hexagonal overlayer with interatomic distances close to the bulk value of the adsorbate appears to form. Another, perhaps more satisfactory interpretation of the LEED patterns yields an overlayer structure with out-of-phase domains, reflecting the remaining strength of the substrate-adatom interaction. In the case of strong adatom-adatom attraction and weak substrate-adatom attraction, one observes the independent superposition of the structures of the pure adsorbate and the pure substrate; i.e., incommensurate structures. Often such dense overlayers have a lattice that is slightly rotated with respect to the substrate lattice. This is called "orientational epitaxy."

Under higher exposure some metals can undergo layer-by-layer growth, while several systems, such as Fe on W(110), form 3-dimensional crystallites. Most cases fall between these two extremes. Comparison of the surface tension of the adsorbate metal and of the substrate metal has failed to explain these phenomena, and up to now there is no simple rule to predict which metal film growth mechanism applies.

When a metal exhibits a (1x1) epitaxial growth despite a substrate lattice constant that differs from its own bulk lattice constant, the overlayer metal can be considerably strained. Therefore, the epitaxial growth must at some point be accompanied by a lattice constant change.

Such a change is probably accompanied by dislocations occurring within a dozen layers from the interface.

Alloy formation is frequently observed with suitable combination of metals, usually at higher temperatures. However very few surface crystallographic data are available on such systems, and a general trend cannot be drawn at this time.

3.2.5. Alloy Surface Structure

About 90 ordered structures of bulk alloys have been reported [5], including both clean and adsorbate-covered surfaces. Alloys have the special property that their surface composition can differ considerably from their bulk composition. Other compounds share this property, but the frequently easy interdiffusion in alloys stands out. Indeed, some recent studies have found substantial surface segregation. In some cases the surface composition can even oscillate from one atomic layer to the next near a surface [26]. Furthermore, adsorbates may radically modify this surface composition. Much work is needed to clarify these issues.

It is found that some alloys retain their bulk ordering at the surface. For instance, Ni_3Al, as well as other Cu_3Au-type alloys, have a (100) face which exhibits the periodicity expected from the alternating bulk stacking of 50-50 mixed NiAl layers and of pure Ni

layers [27]. Other alloys, exemplified by Cu-rich CuAl, are disordered in the bulk, but order at some faces. Thus the (111) face of αCu-16at%Al exhibits a $(\sqrt{3}X\sqrt{3})R30^{o}$ surface periodicity (relative to the (1X1) surface lattice of pure Cu(111) [25]. The other low-Miller-index faces of this alloy do not order.

1.2.2.6. Molecular Adsorbates

Around 390 ordered structures have been reported for the adsorption of molecules [5]. By far the most frequently studied substrates are metals, with only a dozen cases of semiconductors or insulators. Platinum substrates have been most extensively used, due no doubt to their importance in both heterogeneous catalysis and electrochemistry. The most common adsorbates are CO, NO, C_2H_2 (acetylene), C_2H_4 (ethylene), C_6H_6 (benzene), C_2H_6 (ethane), HCOOH (formic acid), and CH_3OH (methanol), reflecting their importance in technological applications.

Most molecular adsorption studies have been carried out near room temperature, with frequent cursory explorations of the higher-temperature behavior. Especially with molecules temperature is a crucial variable given the frequently diverse reaction mechanisms that can occur when molecules interact with surfaces. A number of studies have explored the lower temperatures, especially with the relatively reactive metal

surfaces to the left of the Periodic Table, such as Fe, Mo, and W. At higher temperatures, decomposition of molecules is the rule. With hydrocarbons sequential decomposition has been studied in greatest detail with the help of HREELS vibrational analysis.

The LEED patterns generally reflect disorder at high temperatures. Exceptions occur especially with carbon layers resulting from the decomposition of organic adsorbates: these may form either carbidic chemisorbed layers that are ordered or graphitic layers that have characteristic diffraction patterns.

Ordered LEED patterns for molecular adsorption are frequent at lower temperatures. They can often be interpreted in terms of close-packed layers of molecules, consistent with known Van der Waals sizes and shapes. These ordered structures usually are commensurate with the substrate lattice, indicating strong chemisorption in preferred sites. It appears that many hydrocarbons lie flat on the surface, using unsaturated π-orbitals to bond to the surface [28]. By contrast, non-hydrocarbon molecules form patterns that indicate a variety of bonding orientations. Thus CO is found to strongly prefer an upright orientation. However, upon heating, unsaturated-hydrocarbon adsorbates evolve hydrogen and new species may be formed which bond through the missing hydrogen positions [28]. An example is ethylidyne, CCH_3, which can be formed from ethylene, C_2H_4, upon heating. Ethylidyne has the

ethane geometry, but three hydrogens at one end are replaced by three substrate atoms.

1.2.2.7. Coadsorbed Surface Structures

Over 150 ordered surface structures have been formed upon coadsorption of two or more different species [5]. In general, coadsorbed surface structures may be classified in two categories [29]: cooperative adsorption and competitive adsorption. In cooperative adsorption, the two kinds of adsorbate mix well together and interpenetrate. In competitive adsorption the adsorbates segregate to form separate non-mixed domains. For example, addition of CO to a preadsorbed (2x2) oxygen layer on Pd(111) eventually forms a mixed CO+O phase (cooperative adsorption). On the other hand, addition of O_2 to a preadsorbed CO layer at low coverages on Pd(111) forms separate domains of O and of CO (competitive adsorption). Therefore, in this instance the sequence of adsorption affects the reactivity towards CO_2 formation.

Coadsorption structures have been extensively examined on Rh(111), Pt(111), and Pd(111) using various pairs of adsorbates from the set C_2H_2, C_2H_3, C_6H_6, Na, CO, and NO. Among these, the hydrocarbons and Na transfer electrons to Rh(111) when adsorbed, they are donors. CO and NO have the opposite electron-transfer character, and

are therefore acceptors. It has been observed that long-range ordering of the mixed layer requires the coadsorption of an electron donor with an acceptor. Donor-donor and acceptor-acceptor combinations are either disordered or segregate into separate domains. The combination of donor and acceptor seems to stabilize the mixed cooperative phase. Then each donor adsorbate surrounds itself with acceptors, while each acceptor surrounds itself with donors. This is analogous to the three-dimensional ionic lattices which also exhibit great stability.

As an illustration, on Pd(111) and Pt(111) benzene molecules adsorb in a disordered manner at room temperature. However, addition of CO to these disordered overlayers produces ordered surface structures.

1.2.2.8. Physisorbed Surface Structures

At low enough temperatures most gas-phase species will physisorb on many surfaces. In many instances, the physisorbed state is short-lived (lifetime well below a second), because of a low barrier to a chemisorbed state. With inert gases and with saturated hydrocarbons, however, physisorption is commonplace and stable on many types of substrate. These substrates include metals as well as inert surfaces such as the graphite basal plane. Also, more reactive species such as O_2, CO and NO physisorb and remain stable on the graphite basal plane. We shall focus our discussion on this type of relatively stable

physisorption. Over 60 such ordered structures have been reported [5]. Little is known about the structure of the less stable short-lived physisorbed species, despite their obvious importance as precursors to chemisorbed species.

In physisorption the adsorbate-adsorbate interactions are usually comparable in strength to the adsorbate-substrate interactions, all of which are dominated by the Van der Waals forces. With stable physisorption, there is no significant chemistry leading to bond dissociation to perturb the adsorbates over large ranges of temperature and coverage. One can therefore examine large parts of the phase diagrams of these adsorption systems.

Many phases have been observed in physisorption, and new classes of phases continue to be discovered. There are commensurate and incommensurate phases, disordered lattice-gas and fluid or liquid phases. There are out-of-phase domain structures, including striped-domain phases, pinwheel and herringbone structures, and modulated hexatic reentrant fluid phases, among others. Relative to chemisorption and its more complex interactions, physisorption has the advantage that simpler theories can be set up to describe the phase diagrams. The two-dimensional nature of the problem has especially helped the general theory of phase transitions, because many models can only be solved in two dimensions.

From the point of view of physisorption phases, one should distinguish between the ordering of the positions and of the orientations of the adsorbed species. With spherically symmetrical species like inert gases this is not an issue, but all molecules do offer the additional degrees of orientational freedom, which freeze in at different temperatures than does the positional ordering. This adds considerable richness to the phase diagrams.

The simpler among the observed LEED patterns for physisorbed species can often be easily interpreted in terms of structural models. The known Van der Waals sizes of the species lead to satisfactory structures which are more or less close-packed. This is especially straightforward with inert gases. With molecules, the best structural models usually involve flat-lying species, which are arranged in a close-packed superlattice. The flat geometry provides the greatest attractive Van der Waals interaction with the substrate.

1.2.2.9. High-Miller-Index (Stepped) Surface Structures

Over 380 ordered surface structures have been observed on the high-Miller-index surfaces [5]. Recent interest has focussed on the clean and chemisorbed structure of high-Miller-index semiconductor surfaces. In particular, very interesting reconstructions of the various high-Miller-index Si, Ge and GaAs surfaces have been observed.

Most of the stepped surfaces are observed to have close-packed terraces separated by steps of one atomic height. Many ordered overlayer structures on these one-atomic-height stepped surfaces have been reported. The observed LEED patterns indicate a strong dependence on the width of the terraces. With wide terraces, adsorbates often order as if no steps were present; i.e., as on the low-Miller-index surface. When the terraces become narrow, the adsorbates are strongly affected by the steps. For instance, carbon monoxide adsorbs with (2x2) and $(\sqrt{3}x\sqrt{3})R30^{o}$ patterns on Rh(S)-[6(111)x(100)], which has (111) terraces six atoms wide separated by (100) oriented steps. These two patterns are also observed on Rh(111). But for the case of Rh(331) with (111) terraces three atoms wide, quite different structures for chemisorbed CO have been observed.

Another important observation is that reconstructions of the high-Miller-index surfaces are frequently induced by the adsorption of O_2, H_2, etc. Examples include: ReO_3 compound formation on the oxygen covered Re(S)-[6(0001)x(1676)] surface; new facet formation on the Ni(210) surface after the adsorption of O_2; facet formation due to the decomposition of hydrocarbons on various Pt and Rh high-Miller-index surfaces; and graphite formation or faceting on Pt(S)-[4(111)x(100)] after the total dehydrogenation of ethylene or benzene on this surface. These restructuring phenomena can often be ascribed to the formation of a stable new phase like oxide, carbide, and nitride. The study of the

surfaces of oxide, carbide and nitride solids will help understand the restructuring phenomena observed on the stepped surfaces.

1.3. THREE-DIMENSIONAL SURFACE STRUCTURE DETERMINATION BY LEED

1.3.1 Theoretical Advances

By analyzing LEED intensities it has been possible to determine many surface structures since approximately 1969 [4,6,7]. At first only very simple structures could be handled, such as clean unreconstructed metal surfaces and simple atomic adsorbates thereon. The limiting factor was theory: the multiple scattering of electrons inherent in LEED complicated the numerical simulation of the LEED process, leading to substantial computational times for more complicated structures. Gradually, theoretical methods were introduced that permitted great progress towards the study of relatively complex structures. This includes even the Si(111)-(7x7) structure [30], which until recently was reputed to be unsolvable by LEED.

Types of more complex structures that have now been solved, or are on the verge of being solved, include: stepped surfaces in the clean state or with adsorbates, large-unit cell semiconductor reconstructions and the effect of adsorbates thereupon, overlayers of large molecules, disordered overlayers, defect structures in clean or adsorbate-covered surfaces, and incommensurate overlayers.

Progress has occurred on two fronts. First, computational efficiency has been vigorously pursued. However, with complex structures, the number of unknown parameters to be determined grows rapidly: the traditional search procedures required computation times that were exponential in the number of parameters. Recently, therefore, methods that reduce this exponential barrier have been developed: directed search methods and the direct method.

1.3.1.1. Towards Diffraction from Complex and Disordered Surfaces

The central task in extending LEED to more complex and disordered structures lies in the theory of multiple scattering. Multiple scattering leads to many possible scattering paths and to self-consistency requirements.

Conventional LEED theory [2,3,31,32] has identified the necessary ingredients of an accurate description of multiple scattering. The muffin-tin model is utilized to represent the scattering potential of the surface atomic lattice. A layered structure is often envisaged in LEED to describe a surface. Atomic layers parallel to the surface are defined, in a way appropriate for each particular theoretical method. Usually, a combined-space representation is chosen, in which the wavefield is expanded in terms of spherical waves within those layers, while it is expanded in plane waves in the gaps between those layers.

In the spherical-wave representation it is most common to use free-space Green functions to describe wave propagation from one atom to another. In the plane-wave representation many methods are available to treat multiple scattering. One is the Bloch-wave method with wave-matching across the surface. Another is layer doubling. A popular method is renormalized forward scattering.

The effect of inelastic energy losses, which reduce the elastically surviving flux of electrons, is usually taken into account through a small imaginary part of the scattering potential, or, equivalently, a mean free path length. Finally, all LEED theories include Debye-Waller factors to represent the effects of thermal vibrations.

The new methods introduced for complex and disordered surfaces use the same physical ingredients and many of the same calculational techniques described in this section. The difference often lies in a new packaging of multiple-scattering paths into units that are better adapted to the new tasks. In other cases, some multiple-scattering paths are neglected. Or a linear expansion is carried out to rapidly compute diffraction intensities for slightly distorted geometries.

1.3.1.2. Theoretical Approaches

We shall now describe general strategies that have been proposed to overcome the computational problems of LEED discussed above. We shall also briefly introduce specific methods.

(i) Full Use of Symmetry. A very effective and obvious approach to performing complex structural analyses is to exploit any available symmetries to speed up the calculations. This has been done routinely for many years in the part of the problem that uses the plane-wave representation [3,31], and less frequently wherever the spherical-wave representation is used [33]. In recent years, the latter approach has been applied to great effect. Thus, complex reconstructions have been analysed in considerable detail in this manner. For example, the Au(110)-(1x2) reconstruction was studied down to third-layer relaxations, both perpendicular and parallel to the surface [34]. Even the highly complex Si(111)-(7x7) structure has been analyzed in terms of individual bond lengths, despite its 200 displaced atoms in the (7x7) unit cell [30].

(ii) Cluster Methods. In cluster methods, the spherical-wave representation is used within clusters representing suitable neighborhoods of all inequivalent surface atoms. Each cluster should be large enough to include all significant multiple-scattering paths which pass through the surface atom at its center. In general, the clusters based on different atoms overlap each other.

The problem is hereby reduced to solving the multiple scattering within each cluster and then combining the individual results. In this way, the computing time is made proportional to the number of translationally inequivalent surface atoms, a great improvement over their second or third power. But it does remain proportional to a high power of the number of atoms within each cluster: therefore, the cluster must be chosen rather small, including only near neighbors.[35,36]

A related approach is the one-center expansion [37], in which the spherical-wave scattering properties of an entire cluster are obtained self-consistently and are then available for calculating plane-wave diffraction in many diffraction conditions. The approach is made efficient by breaking down the clusters into concentric shells and separating the problem of the scattering by individual shells from that of the scattering by the assembly of shells [38,39]. A variant of this method has been developed for steps, or, more generally, for "linear defects" [40]. Here, cylindrical waves are used to describe the multiple scattering within individual chains of atoms, which are chosen parallel to the linear defect. These chains are then combined into three-dimensional surfaces (this method has close analogies with the earlier "chain method" developed for medium- and high-energy electron diffraction [41]).

Another cluster method was proposed by Marcus et al [42]: it sums explicitly over scattering paths limited in length by the mean free path.

These methods exhibit the common feature that the computing time scales in simple proportion to the number of inequivalent surface atoms.

(iii) Reducing Multiple-Scattering Paths. Another strategy consists in identifying and ignoring large classes of paths that contribute only weakly to the diffracted intensities. In dense metal surfaces, for which the conventional LEED theory was developed, it is difficult to find classes of weak paths. But in many other materials, multiple scattering is much less important. For example, aluminum and silicon are more "kinematical" materials as far as LEED is concerned. And so are many other open-lattice semiconductors, as well as many low-density materials and overlayers, especially molecular overlayers.

Weak multiple-scattering paths can be eliminated in several ways. First, one may simply shrink the size of the above-mentioned clusters, within which one allows multiple scattering around each atom. In this manner, the individual cluster calculation is made much faster. This approach was introduced by Moritz et al [36]. It stands the best chance of being reasonably accurate in loosely-packed materials. Thus, semiconductors and molecular materials are good candidates for this treatment.

It is also possible to prevent long distances between successive scatterings in a multiple-scattering path: far fewer paths are then

allowed. Thus, in the method called "near-neighbor multiple scattering" (NNMS) [43,44], a multiple-scattering path is only allowed to consist of short "hops" between nearest neighbors (a string of short hops may lead as far away as the mean free path allows). This approach does not reduce the scaling power of the computing time dependence on N, the number of atoms in a unit cell or cluster, but it does reduce its prefactor considerably.

A simple but very effective variant is "kinematic sublayer addition" (KSLA) [45]. It applies to the case where the clusters are disjoint, i.e. no multiple-scattering path can hop from one cluster to another. An example is molecular layers, where the hop from an atom in one molecule to an atom in another molecule is often too long to provide a significant contribution to intensities. In that case the scattering properties of the separate molecules can be calculated independently. They then can be kinematically combined and recombined for many different relative positions of the different molecules.

(iv) Beam Set Neglect. Next we consider a method that is plane-wave oriented. Thus, the intention is to identify and eliminate sets of plane waves that do not contribute significantly.

The "beam set neglect" (BSN) method [46] applies to overlayers or reconstructed layers with a superlattice or a disordered lattice on a

perfect substrate. It recognizes the fact that only a very limited set of plane waves (beams) contribute significantly to the detected intensities: many sets of beams can be neglected in the calculation. As a result, the dependence of the computation cost on the unit-cell area A and the energy E fall from the second or third power to no dependence. In other words, the computation cost can be made independent of the energy, the unit-cell area or the presence of disorder. This approach works also for disordered and incommensurate overlayers, as described below. BSN can be very effectively combined with cluster methods, in particular the KSLA method.

(v) Tensor LEED, directed search and direct methods. A third basic approach is to approximate LEED intensities as being linear expansions from those for a nearby surface geometry that was treated exactly. Thus, one computes exactly the LEED intensities for a given reference structure, preferably a simpler one: for example, a highly-symmetrical or undistorted structure. Then, the intensities for a somewhat deviating structure would be computed, using a linear expansion in terms of the structural parameters. This yields excellent computation times, especially if many deviating structures around the reference structure are explored, because the linear expansion itself is a very simple operation. This is the philosophy of tensor LEED [47], which has already been applied to periodic or disordered surface reconstructions and to disordered overlayers that induce substrate distortions. The tensor LEED

approach appears to give excellent results for structural distortions less than about 0.4Å.

Using tensor LEED, one can easily develop an automated structure search procedure, called directed search [48]. One makes an initial guess at the structure (the reference structure), which requires a fully-dynamical calculation. Then, as many structural parameters as one wishes can be relaxed and adjusted to experiment, by means of the very efficient tensor LEED expansion. This can be combined with a steepest-descent algorithm which automatically finds a nearby minimum in an R-factor (that measures the disagreement between theory and experiment). If no nearby minimum is found within about 0.4Å, the method points in the direction where one can be found, and the procedure can be restarted. Thereby, we have a scheme which requires a computation time proportional to the number of unknown parameters, rather than exponential in that number, an immense improvement over conventional search strategies. However, the R-factor minimum found by directed search cannot be guaranteed to be the global minimum; i.e., may not always give the correct answer; this is a limitation of any procedure involving diffraction.

Another application of tensor LEED is the direct method [49]. Again a reference structure is guessed. If this structure is close to the actual structure, inversion of the tensor(s) of the tensor LEED

method can in principle predict the actual structure directly. All that is required is a relatively small amount of experimental data (less than normally used in LEED analyses). The direct method has been shown to work well if the guessed reference structure is rather close to the actual structure: structural parameters should be guessed to better than about 0.1Å. If this condition is not satisfied, an iteration procedure may be applied, solving the structure stepwise. Again the computational time is no longer exponential in the number of unknown parameters. Additionally, this direct method can deliver information about anharmonic vibrations of the surface atoms.

1.3.1.3. Disorder and Diffraction

Many surfaces are disordered. The LEED theory has been developed to solve the structure of some of these very interesting surfaces, principally those that have lattice-gas disorder [50-52]: an important example is the case of an atomic or molecular overlayer on a perfectly periodic substrate, all adsorbates occupying identical sites on the substrate. For instance, we may consider a disordered layer of oxygen on Ni(100), with all oxygen atoms bonded identically in four-fold hollow sites. Thus, we have identical short-range order, but no long-range order.

To understand how order and disorder affect the diffraction of

electrons by a surface, we make a fundamental distinction between "lattice" and "basis." For an ordered surface, the lattice describes its periodicity; i.e., the shape, size and orientation of the unit cell, but not its contents. Thus, the lattice describes only the long-range structure. It is responsible for the presence of sharp LEED beams and spots in the case of an ordered surface. The spot positions are not affected by multiple scattering. We may call this lattice-induced contribution the "structure factor."

The "basis" is the set of atoms that is contained within any unit cell, together with their individual positions and scattering properties. The basis therefore describes the short-range order. The intensities of the LEED beams are governed by the basis. These intensities are strongly affected by multiple scattering. They depend in particular on the relative positions of the basis atoms through the multiple scattering. Therefore, intensities are often said to be "dynamical." We may call this basis-induced contribution the "form factor."

Thus, the diffraction pattern is primarily determined by long-range order, while the diffraction intensity is primarily determined by short-range order. One may qualitatively view the observed LEED intensities as the product of the smoothly varying basis-induced form factor and the lattice-induced structure factor. This product

relationship becomes exact for the dilute lattice gas. In fact, most practical disordered overlayers are close enough to the limit of the dilute lattice gas for this product relationship to hold.

Thus, for a lattice gas, the final pattern can be viewed as the product of a kinematic structure factor reflecting the long-range disorder and a dynamical form factor reflecting the local short-range order. If the short-range structure is to be found, the unknown structure factor must be first removed (which is easy to do for a purely two-dimensional disorder). Then a LEED calculation that allows all electron exit directions can simulate the experimental data and lead to all the desired short-range structural information.

Two schemes for such LEED calculations are in use. The first, more exact scheme takes a cluster approach and is quite similar to the NEXAFS (XANES) problem [50,51]. This three-step approach first allows a planar LEED beam to scatter in all possible ways through the substrate until it first reaches a disordered adsorbate. This wave is then expressed in spherical waves which are allowed to scatter in all possible ways through the surface until their last encounter with the disordered adsorbate. Finally, these spherical waves are propagated again as a plane wave in all possible ways through the substrate to the detector.

The second, less accurate, but speedier method uses the

beam-set-neglect approach [50,52]. In the second step above, the spherical waves are replaced by the two sets of plane waves defined in the beam set neglect method, and the three steps can then be combined into a single efficient plane-wave step identical to conventional LEED methods.

1.3.1.4. Incommensurate Overlayers

Beam set neglect has provided a new solution to the problem of calculating diffracted intensities from incommensurate overlayers [53]. By incommensurate we mean that the overlayer has a two-dimensional periodic lattice which is independent of that of the substrate. This situation is common with overlayers that are strongly cohesive and can ignore the periodicity of the substrate on which they lie; for instance, graphite and oxides or other strong compounds form overlayers with their own bulk lattice, which in general does not match that of the substrate. By using exactly the same arguments as above for ordered and disordered overlayers, one can easily show that acceptably accurate calculations can be performed with just the two sets of beams defined earlier. Again, the effect is to ignore weak third- and higher-order multiple-scattering paths. This approach has been applied to the structure determination of a graphite layer grown from hydrocarbon decomposition on a Pt(111) substrate [53].

1.3.2. Clean Surface: Mainly Inward Relaxations

Surface atoms have a highly asymmetrical environment: they have many neighbors toward the bulk and in the surface plane, but none outside the surface. This anisotropic environment forces the atoms into new equilibrium positions. For clean unreconstructed surfaces, there is generally a contraction of bond lengths between atoms in the top layer and the second layer under the surface, relative to bond length value in the bulk [4,6,7]. This relaxation in the topmost interlayer spacing is larger the more open (or rougher) is the surface; i.e., the fewer neighbors the surface atom has. The closest packed surfaces, such as fcc(111) and fcc(100), show almost no relaxation; there may even be a very slight expansion for Pd and Pt(111). Large inward relaxations occur by contrast at surfaces like fcc(110), with interlayer spacings contracted by about 10%. The contractions are material dependent, Pb(110) showing a particularly large value of 16%. Jona and Marcus [54] have plotted the percent relaxation as a function of the inverse of the packing density, which is called the roughness factor, see Figure 1.6. The trend of larger relaxation with fewer neighbors around the surface atoms is clearly discernable.

It should be recalled that interatomic distances for diatomic molecules are much shorter than bond distances in solids where atoms have many more nearest neighbors [18]. The surface atoms may be viewed as

having a chemical environment that is between a diatomic molecule and an atom in the bulk of the solid.

For stepped and kinked surfaces the atoms at the edges are more exposed and are expected to exhibit large relaxations with the effect of causing a partial smoothing at these rough surface sites. There is very little quantitative information documenting the magnitude of relaxation at these defect sites but the available experimental information [54] does suggest relaxations at the step edges that are comparable to those shown in Figure 1.6 for rough surfaces.

Relaxations of interlayer spacings occur also below the second layer [54]. The amplitudes of these relaxations decay approximately exponentially with depth. The decay appears to be related more to physical depth than to interlayer spacing, since higher-Miller-index surfaces with smaller interlayer spacings show relaxations that propagate more layers down, but not deeper as measured in Ångstrom.

Relaxations parallel to the surface are also possible [54]. These occur when the surface has a relatively low two-dimensional symmetry. For example, atoms at step edges will tend to relax sideways toward the upper terrace of which they are a part. Such sideways relaxations can also propagate deeper below the surface.

1.3.3. Clean Surface Reconstructions

A fair proportion of clean surfaces adopts non-bulk lattices; that is, they reconstruct [4,6,7]. This is usually accompanied by the appearance of a superlattice due to a different two-dimensional periodicity relative to the ideal truncation of the bulk lattice.

Various types of reconstruction occur, each being caused by a different mechanism. A mild form consists of rehybridization without bond breaking. In GaAs(110), for example, bond angles change substantially, with only minor changes in bond lengths, compared to the bulk lattice. Similar is the displacive reconstruction of W and Mo(100) in which the metal atoms move slightly to form zigzag rows of bonded atoms parallel to the surfaces [55]. A type of reconstruction that maintains bulk sites is exemplified by the missing-row structure of Ir, Pt, and Au(110); here half the surface atoms are "missing" from the ideal structure (some bond length relaxations like those in clean unreconstructed metal surfaces also take place). More drastic reconstructions are seen at the Ir, Pt, and Au(100) surfaces [19]. In this case the bond length between atoms in the topmost layer shrinks enough to cause a collapse of the entire top layer into a nearly hexagonal close-packed layer, which rests as well as it can on the square-lattice second metal layer. Such large-scale rebonding is common at semiconductor surfaces and can involve atoms in deeper layers as well.

It appears that the main driving mechanism for semiconductor reconstruction is the minimization of the number of dangling bonds. Si and Ge provide numerous examples of complex reconstructions. The Si(111)-(7x7) structure combines adatoms, dimers and in one half of the (7x7) unit cell a stacking fault to drastically reduce the number of dangling bonds.

1.3.4. Surface Alloys and Compounds

The clean surface alloys fall into two main categories: those for which the bulk alloy is ordered and those for which it is disordered.

It appears that the surface structures of ordered bulk alloys are also ordered and maintain the bulk concentration. NiAl and Ni_3Al in particular have been extensively studied and found to satisfy this principle. Some bond length relaxations are apparent. At least for $Ni_3Al(100)$ they are consistent with the idea that the smaller Ni atoms sink into the surface more than the larger Al atoms do [27].

With disordered bulk alloys, the surface is most often also disordered, but surface segregation can be very marked and can be strongly layer-dependent, with the possibility of an oscillating layer-by-layer concentration. For instance different crystallographic faces of the Pt_xNi_{1-x} alloy have been found to exhibit very different segregation behavior as well as a strong layer dependence [26].

In at least one case, the (111) surface of Cu_xAl_{1-x} with x=84%, surface ordering despite a disordered bulk is observed. In this case the first layer contains 33% of Al (double the bulk concentration), ordered in a $(\sqrt{3} \times \sqrt{3})R30^0$ structure, while the second layer is probably nearly pure Cu [25].

Bulk compounds like oxides, carbides, sulfides and semiconductors, often maintain the bulk composition at the surface (together with bond angle changes in the semiconductor surfaces). But there are numerous exceptions. Thus, iron oxides can have a deviating surface composition. In the (111) faces of GaAs, GaP, and other such semiconductors, a deficiency of Ga is found which leads to a (2x2) reconstruction.

1.3.5. Surface Crystallography of Adatoms

1.3.5.1. Adsorption sites

The simple atomic adsorption structures on metal surfaces are characterized by the occupancy of high-coordination sites [4,6,7]. Thus Na, S, and Cl overwhelmingly adsorb over "hollows" of the metal surface, bonding to as many metal atoms as possible. The situation is slightly more complicated with the smaller adsorbates, H, C, N, and O. Although high coordination is still preferred, the small size of these atoms often

allows penetration within or even below the first metal layer. The penetration can be interstitial (as in metals) or substitutional (as often in semiconductors and compounds). In either case the surface can reconstruct as a result, especially at higher coverages. For instance, a monolayer of N penetrates into interstitial octahedral sites between the first two layers of Ti and Zr(0001) with minimal distortion of the metal lattice. Both C and N burrow themselves within the hollow sites of the Ni(100) surfaces so as to be almost coplanar with the topmost Ni atoms. The nearest Ni atoms are also pushed sideways by perhaps 0.4Å, forming a good example of adsorbate-induced reconstruction (see below).

1.3.5.2. Bond Lengths

The observed bond lengths between adatoms and substrate atoms generally fall well within 0.1Å of comparable bond lengths measured in bulk compounds and molecules. Pauling-type rules are found to apply well to describe these bond lengths [56]. In a few cases the accuracy is sufficient to detect significant variations in bond lengths. For example, when the surface coverage of Cs is varied from 1/3 to 2/3 monolayers on Ag(111), the Ag-Cs bond length is found to change from 3.20Å to 3.50Å [57]. This illustrates an expected effect of mutual interactions between adsorbates: the denser the adsorbate layer, the weaker the individual adatom-substrate bonds.

1.3.5.3. Adatom Induced Outward Relaxation

When atoms adsorb on an inward relaxed clean surface and form chemical bonds, the surface atoms are placed in a different chemical environment. Upon adsorption, any clean surface inward relaxation is generally reduced as the surface atoms of the substrate move back towards the ideal bulk-like position or even beyond (see Table 1.2). Relaxations of deeper interlayer spacings are also much reduced upon adsorption [20].

Good examples of the outward relaxation of interlayer spacings are provided by atomic adsorption on the (110) surfaces of nickel and other fcc metals. The clean (110) surfaces typically exhibit contractions by about 10% (0.1 to 0.15Å) in the topmost interlayer spacing relative to the bulk value. Upon adsorption these contractions are reduced to less than 3 to 4% (0.03 to 0.05Å), often indistinguishable from the bulk value.

1.3.5.4. Adsorbate-Induced Surface Restructuring.

The adsorption of atoms may displace substrate atoms parallel to the surface to provide better adsorbate-substrate bonding [20]. This is

Table 1.2. Adsorbate-induced reductions of clean-surface spacing relaxations. Shown are the expansions of the topmost (and second, when available) metal-metal interlayer spacings, from the clean surface relaxations, in percent of the bulk spacing value. Thus, "10% from -5%" would imply that the clean surface has a -5% contraction relative to the unrelaxed bulk spacing, and the adsorbate-covered surface has an expansion of -5+10 = +5% relative to the unrelaxed bulk spacing.

Surface	Description	Reference
Fe(100)-c(2x2)-N	11.5% from -1.4%	a
Fe(100)-(1x1)-O	9% from -1.4%	b
Fe(100)-c(2x2)-S	3% from -5%	c
Co(100)-c(2x2)-O	4% from -4%	d
Ni(110)-(2x1)-2H	4%(1.5%) from -8.5% (3.5%)	e
Ni(100)-c(2x2)-O	8% from -5%	f
Ni(110)-c(2x2)-S	19% (-7%) from -8.5% (3.5%), with buckling by 11% of the second Ni layer	g
Ni(100)-c(2x2)-S	4% from 0%, with some buckling of the second Ni layer	h
Cu(110)-"(1x1)"-H	9% (0%) from -8% (2.5%)	i
Cu(100)-c(2x2)-Cl	2.5% from 0%	j
Cu(100)-c(2x2)-N	8% from 0%	k
Mo(100)-c(2x2)-N	9.5% from -9.5%	l
Mo(100)-c(2x2)-S	7% from -9.5%	m
Mo(100)-(1x1)-Si	9.5% from -9.5%	n
Rh(110)-(1x1)-2H	5% from -7%	o,p
Rh(110)-c(2x2)-S	3% from -3%	q
Pd(110)-(2x1)-2H	4% (2%) from -6% (1%)	p
Pd(111)-($\sqrt{3}$x$\sqrt{3}$)R30^{o}-CO	5% from 1%	r
Ag(110)-(2x1)-O	7% from -7%	s
W(100)-(1x1)-2H	4% from -6%	t
Ir(110)-(2x2)-2S	9% (10%) from -12%) (both the clean and the S-covered surface have the missing-row reconstruction)	u

a. R. Imbihl, R.J. Behm, G. Ertl and W. Moritz, Surface Sci. 123, 129 (1982).
b. J. Sokolov, F. Jona and P.M. Marcus, Europhysics Lett. 1, 401 (1986).
c. X.S. Zhang, L.J. Terminello, S. Kim, Z.Q. Huang, A.E. Schach von Wittenau and D.A. Shirley, submitted to Phys. Rev. B; Z.Q. Wang, Y.S. Li, F. Jona and P.M. Marcus, Sol. St. Commun. 61, 623 (1987).
d. A. Ignatiev, B.W. Lee and M.A. Van Hove, Proc. 7th International Congress and 3rd International Conference on Solid Surfaces, eds. R. Dobrozemsky, F. Rüdenauer, F.P. Viehböck and A. Breth, Vienna (1977).
e. W. Reimer, V. Penka, M. Skottke, R.J. Behm, G. Ertl and W. Moritz, Surface Sci. 186, 45 (1987).
f. J.W.M. Frenken, J.F. van der Veen and G. Allan, Phys. Rev. Lett. 51, 1876 (1983).
g. R. Baudoing, Y. Gauthier and Y. Joly, J. Phys. C18, 4061 (1985); S.W. Robey, J.J. Barton, C.C. Bahr, G. Liu and D.A. Shirley, Phys. Rev. B35, 1108 (1987).
h. J.J. Barton, C.C. Bahr, S.W. Robey, Z. Hussain, E. Umbach and D.A. Shirley, Phys. Rev. B34, 3807 (1986).
i. A.P. Baddorf, I.-W. Lyo, E.W. Plummer and H.L. Davis, J. Vac. Sci. Technol. A5, 782 (1987).
j. F. Jona, D. Westphal, A. Goldmann and P.M. Marcus, J. Phys. C16, 3001 (1983).
k. H.C. Zeng, R.N.S. Sodhi and K.A.R. Mitchell, Surface Sci. 188, 599 (1987).
l. A. Ignatiev, F. Jona, D.W. Jepsen and P.M. Marcus, Surface Sci. 49, 189 (1975).
m. L.J. Clarke, Surface Sci. 102, 331 (1981).
n. A. Ignatiev, F. Jona, D.W. Jepsen and P.M. Marcus, Phys. Rev. B11, 4780 (1975).
o. W. Nichtl, N. Bickel, L. Hammer, K. Heinz and K. Müller, Surface Sci. 188, L729 (1987).
p. M. Skottke, R.J. Behm, G. Ertl, V. Penka and W. Moritz, J. Chem. Phys., 87, 6191 (1987).
q. S. Hengrasmee, P.R. Watson, D.C. Frost and K.A.R. Mitchell, Surface Sci. 92, 71 (1980).
r. H. Ohtani, M.A. Van Hove and G.A. Somorjai, Surface Sci. 187, 372 (1987).
s. A. Puschmann and J. Haase, Surface Sci. 144, 559 (1984).
t. M.A. Passler, B.W. Lee and A. Ignatiev, Surface Sci. 150, 263 (1985).
u. C.M. Chan and M.A. Van Hove, Surface Sci. 183, 303 (1987).

well illustrated by the effect of carbon adsorbed on Ni(100) [58]. The adatom occupies a four-fold site. By expanding the site by the movement of neighboring nickel atoms, the carbon atom penetrates the nickel surface so as to bond not only to the four first-layer nickel atoms but also to a Ni atom in the second metal layer. The surrounding metal lattice cannot accept a corresponding compression at a half-monolayer coverage and instead forces a rotation of the square of four Ni atoms about the surface normal. Thereby, the average metal density in the top layer is kept constant.

Oxygen on Ni(100) also induces substrate relaxations [59,60]. In the c(2x2) and p(2x2) structures, a buckling appears in the second Ni layer, while the first Ni layer moves slightly outward relative to the clean surface. The second-layer Ni atom directly below an oxygen atom (which is centered over a hollow site) is pushed down, away from the oxygen atom.

Another example of adsorbate-induced surface restructuring is provided by sulfur on Fe(110) [61]. The clean Fe(110) surface provides two-fold and three-fold coordination sites for adsorption. Sulfur maximizes its coordination number to nearly four by distorting the two-fold coordination site into a nearly square "hollow" site.

Sulfur can restructure Mo(100) as well [62]. At a half-monolayer coverage, sulfur forms a c(2x2) structure. However, the sulfur atoms are not located exactly over hollow sites, but about 0.2Å away in asymmetrical positions. The first Mo layer is restructured, showing complex lateral displacements. It is likely that the lateral displacements of both the sulfur and first Mo layers have random orientations, resulting in many local configurations.

The energy needed for surface restructuring is paid for by the increased bond energies between the adsorbed atom and the substrate. Therefore, such surface restructuring is expected only upon chemisorption where the adsorbate-substrate bonds are similar to the bond energies between the atoms in the substrate. This is clearly the case for the adsorption of carbon, oxygen, and sulfur on many transition metals.

The geometry of the restructured adsorption site provides evidence for "clustering"; i.e., the formation of a 4-6 atom cluster that includes the adsorbed atom and its nearest neighbors. One interesting example of how the long range order at the clean substrate surface breaks up into small clusters upon chemisorption is oxygen on the W(100) surface [51]. When clean, the W(100) reconstructed surface is characterized by long zigzag chains of surface metal atoms. When oxygen is adsorbed, at low coverage, each oxygen atom occupies a hollow site and pulls the four

nearest W atoms inward toward the oxygen position. Thereby a 5-atom cluster is created that is separated laterally from other atoms on the surface.

Often, the chemisorption of atoms removes surface reconstruction and produces a more bulk-like surface structure. Among the most frequently studied examples of this type of adsorbate-induced restructuring are those of hydrogen that removes the reconstruction of clean Si(111) and diamond C(111) and of carbon that removes the reconstruction of Ir and Pt(100).

1.3.6. Surface Crystallography of Ordered Molecules

1.3.6.1. Carbon Monoxide and Nitric Oxide Adsorption

Detailed LEED studies of CO and NO have been performed for a dozen surface structures [63]. They have confirmed the site assignments based on vibrational frequencies, as originally derived for metal-carbonyl and similar complexes. On many metals, CO prefers low-coordination sites at low coverages, e.g. linear coordination at top sites for CO on Pt(111). At higher coverages coordination generally increases, towards two-fold bridge sites and three-fold hollow sites (but apparently never four-fold hollow sites). The metal-C bond length has been found to increase with

coordination, as has the C-O bond length, again in agreement with metal-carbonyl complexes, confirming the C-O bond weakening implied by the decreasing vibration frequency.

At high coverages, crowding occurs and part of the CO and NO molecules have to settle for lower-symmetry sites. For instance, at 3/4-monolayer coverage on Rh(111), one third of the adsorbed CO occupies bridge sites, while the remainder are pushed off the top sites by about 0.4 Å [44]. NO in the same circumstances does the same thing, but the displacement away from the top site is smaller [64], in accord with the smaller packing diameter of this molecule. There is no clear indication for CO tilting away from the surface normal in these structures, but tilting by up to 20^{o} has been observed by LEED and photoemission in several other close-packed structures [65-67].

1.3.6.2 Surface Crystallography of Organic Molecules

Much effort has been concentrated in our laboratory to explore the structure of small organic molecules (with six carbon atoms or less). The substrates that were utilized were mostly noble metals (platinum, rhodium, and palladium) with their low Miller index flat orientations ((111) and (100)). The studies focussed on adsorbed monolayers of olefins and of benzene that chemisorb near 300 K and at low pressures and

order readily on these surfaces under appropriate circumstances. There are two general properties that emerged from these studies [28]: a) thermal activation and b) organo-metallic cluster-like bonding. Thermal activation means selective and sequential bond breaking in the chemisorbed molecules (C-H or C-C bonds) that occur at well defined temperatures leaving behind a partially dehydrogenated organic fragment molecule. Organo-metallic cluster-like bonding means that the surface structure of the adsorbed molecule or molecular fragment is very similar, or identical to the structure of multinuclear organo-metallic compounds taht contain at least three metal atoms per molecule [68].

Perhaps the best way to demonstrate the structural and bonding properties of organic molecules on metal surfaces is to describe in some detail the surface chemical behavior of ethylene and benzene.

Ethylene adsorbs intact at low temperatures on metal surfaces. Upon heating, it loses hydrogen sequentially. Between the different temperatures at which hydrogen desorption occurs, stable partially dehydrogenated intermediates exist. At low temperatures the C-C bond of the intact ethylene is parallel to the metal surface. Such structures have analogues among the organo-metallic cluster compounds. As one increases the temperature to 300 K, ethylidyne forms by elimination of one hydrogen atom per molecule. It has the stoichiometry C_2H_3 and a

C-C bond that is perpendicular to the surface. On the (111) surface of platinum, rhodium and other transition metals this molecule sits in a 3-fold site and its C-C bond is elongated to between a single and double bond. Many organometallic multi-nuclear clusters exist with the same structure.

Increasing the temperature converts the ethylidyne molecules to C_2H and CH species. Several organometallic multi-nuclear complexes exist with these structures, again indicating that the adsorbed organic fragment on surfaces have structures identical to those in multi-nuclear organometallic clusters.

The sequential bond breaking of ethylene has been observed on many single crystal surfaces of transition metals. The breaking of C-H or C-C bonds occurs sequentially in a narrow temperature range. The product molecules that form are very similar to those found on the noble metal surfaces. However, the more open the surface or the rougher its surface structure, the lower is the temperature at which the scission of a given bond takes place. Thus, the rougher the surface, the more readily it carries out chemical rearrangements. This is easily seen by comparing ethylene bond breaking on Ni[5(111) x (111)] and Ni(111) surfaces. On the stepped surface bond rearrangement occurs below 150 K while it occurs only around 300 K on the flat low Miller index crystal face.

Benzene adsorbs parallel to fcc(111) surfaces and probably on many other flat surfaces [63]. The adsorption site is variable. On Pt(111), the molecule centers itself over a bridge site, whether benzene is mixed with CO or not. On Rh(111), the same site is found for a pure benzene layer, but a 3-fold hollow site emerges in the presence of coadsorbed CO. On Pd(111), in the presence of CO, the 3-fold site is also found.

The height of the benzene carbon ring over the metal surface varies with the metal (in the presence of coadsorbed CO): it is largest on Pd(111), smallest on Pt(111) and intermediate on Rh(111). Another, more remarkable, trend is an expansion of the carbon ring radius: the radius is close to the gas-phase value (1.40 Å) on Pd(111), larger by about 0.35 Å on Pt(111) and intermediate on Rh(111). Furthermore, there appears to be a reduction of the rotational ring symmetry from 6-fold, due to long and short C-C bonds: the symmetry is 3-fold (with 3 mirror planes) when the adsorption site is a hollow site, while it becomes 2-fold (with 2 mirror planes) over a bridge site.

1.3.6.3. Coadsorption

Carbon monoxide induces order in adsorbed benzene overlayers on Rh(111) and Pt(111) surfaces [29]. Carbon monoxide induced ordering has also been observed for a wide variety of adsorbates [acetylene,

ethylidyne ($\equiv CCH_3$), propylidyne ($\equiv CHCH_2CH_3$), benzene, fluorobenzene, sodium, potassium, and hydrogen] on several metal surfaces [Rh(111), Pt(111), Pd(111), Rh(100), Ru(001), Ni(100), and Ni(110)]. In these cases, the coadsorption of CO with another adsorbate results in the formation of new ordered surface structures different from those formed when either CO or the other adsorbate are present alone on these surfaces. The formation of these ordered, coadsorbed structures provides an excellent opportunity for studying the interaction between coadsorbed atoms and molecules under conditions where the relative geometry and stoichiometry can be established.

The CO induced ordering with several coadsorbates - sodium, benzene, fluorobenzene, and ethylidyne - on the Rh(111) crystal surface and the reduction in the C-O stretching frequency can be correlated with the surface dipole moments of the adsorbates. Here, the surface dipole moments are determined by measuring work function changes as a function of adsorbate coverages. CO induced ordering occurs when CO is coadsorbed with an adsorbate (like NO) that has a surface dipole moment oriented opposite to that of adsorbed CO, while disorder or segregation occurs when CO is coadsorbed with an adsorbate that has a similarly oriented dipole moment. We also find that NO, a ligand chemically similar to CO, has a surface dipole moment opposite that of ethylidyne when coadsorbed in the c(4x2) - NO + ethylidyne structure. Further, the magnitude of

the reduction in the C-O stretching frequency appears to be directly related to the surface dipole moment of the coadsorbate.

For several of the CO coadsorbed structures, dynamical LEED analyses have determined the adsorption geometries of the coadsorbed molecules, including the bond lengths and bond angles [4]. In all the CO coadsorbed structures on Rh(111) solved by LEED, the adsorption site of CO is an hcp hollow site, where one second layer rhodium atom sits below the three-fold site occupied by the CO molecule.

1.4 FUTURE TRENDS

Perhaps one of the most pervasive observations of recent LEED surface crystallography studies is adsorbate induced restructuring and the formation of cluster-like bonding [68] between the adsorbate and substrate atoms. As a result, structure determinations have to carefully probe the locations of both the adsorbed and the substrate atoms. Many of the surface structures reported earlier will have to be reevaluated in light of the possibility of adsorbate induced restructuring. The tensor-LEED technique that was developed recently permits probing a large variety of structural possibilities with relatively small computational effort [48].

The structure analysis of disordered surface monolayers is another area that will be expanding rapidly in the near future. One can minimize the experimental effort to prepare these layers. In addition it is likely that the adsorption site and bonding could be different in the absence of long range order.

Organic surface chemistry is an important, rapidly expanding field of surface crystallography. Monolayers of organic molecules with increasing size and molecular complexity will be studied. Multilayers of ordered organic or molecular crystals will be studied as digital LEED removes the radiation damage that would disorder or decompose these molecular systems.

The structure of stepped surfaces, rougher, more open surfaces will be the subject of structural studies, since these exhibit much higher chemical activity for adsorbate bond breaking or for catalytic reactions than flat, close-packed surfaces.

The surface structures of polyatomic solids, oxides, sulfides, silicates, and carbonates will be studied as permitted by the ease of surface structure calculations using reliable approximate methods.

The structure of metals and other adsorbates on semiconductors

will increasingly be investigated, in large part due to the technological importance of heterojunction interfaces.

The ever expanding database generated by surface structure studies will improve our insight into the nature of the surface chemical bond and accelerate the developments of many applications of surface science from heterogeneous catalysis to biopolymeric surfaces.

ACKNOWLEDGEMENTS

This work was supported in part by the Director, Office of Energy Research, Office of Basic Energy Sciences, Materials Sciences Division of the U.S. Department of Energy under Contract No. DE-AC03-76SF00098. Supercomputer time was also made available by the Office of Energy Research of the U.S. Department of Energy. A part of the theoretical development was funded by the Army Research Office. Many colleagues have contributed significantly to our work described in this text: J.J. Barton, B.E. Bent, G.S. Blackman, C.-M. Chan, P. de Andres, Z.P. Hu, R.Q. Hwang, D. Jentz, C.-T. Kao, D.G. Kelly, R.J. Koestner, R.F. Lin, C.M. Mate, D.F. Ogletree, H. Ohtani, J.B. Pendry, P.J. Rous, D.K. Saldin, E. Sowa, A. Wander, and M.L. Xu.

REFERENCES

1. G.A. Somorjai, Chemistry in Two Dimensions; Cornell University Press: Ithaca, NY, 1981.

2. M.A. Van Hove, S.Y. Tong, Surface Crystallography by Low Energy Electron Diffraction: Theory, Computation and Structural Results; Springer: Heidelberg, 1979.

3. M.A. Van Hove, W. H. Weinberg, C.-M. Chan, Low-Energy Electron Diffraction: Experiment, Theory, and Structural Determination, Springer-Verlag, Berlin (1986).

4. J.M. MacLaren, J.B. Pendry, P.J. Rous, D.K. Saldin, G.A. Somorjai, M.A. Van Hove and D.D. Vvedensky, "Surface Crystallographic Information Service: A Handbook of Surface Structures," D. Reidel (Dordrecht, Holland) 1987.

5. H. Ohtani, C.-T. Kao, M.A. Van Hove, G.A. Somorjai, Progr. Surf. Sci. 23, 155 (1987).

6. P.R. Watson, "Critical Compilation of Surface Structures Determined by LEED Crystallography," J. Phys. Chem. Ref. Data 16, 953 (1987), and J. Phys. Chem. Ref. Data, in press.

7. M.A. Van Hove, S.W. Wang, D.F. Ogletree and G.A. Somorjai, Adv. Quantum Chem. 20, 1 (1989).

8. C.S. Fadley, in "Synchrotron Research: Advances in Surface Science," Ed. R.Z. Bachrack, Plenum (New York) 1990, in press.

9. P.H. Citrin, J. Phys. (Paris), Colloque C8, 437 (1986).

10. J.E. Rowe, in "Synchrotron Research: Advances in Surface Science," Ed. R.Z. Bachrach, Plenum (New York) 1990, in press.

11. J.F. van der Veen, Surf. Sci. Rep. 5, 199 (1985).

12. Proc. 4th Int'l Conf. on STM/STS, J. Vac. Sci. Technol. A8, 153-726 (1990).

13. R. Feidenhans'l, Surf. Sci. Rep. 10, 105 (1989).

14. D.F. Ogletree, R.Q. Hwang and G.A. Somorjai, to be published.

15. E.A. Wood, J. Appl. Phys. 35, 1306 (1964).

16. B. Lang, R. W. Joyner and G. A. Somorjai, Surf. Sci. 30, 454 (1972).

17. M. A. Van Hove and G. A. Somorjai, Surf. Sci. 92, 489 (1980).

18. L. Pauling, The Nature of the Chemical Bond, 3rd Ed., Cornell University Press, New York (1960).

19. M.A. Van Hove, R.J. Koestner, P.C. Stair, J.P. Biberian, L.L. Kesmodel, I. Bartos and G.A. Somorjai, Surf. Sci. 103, 189 and 218 (1981).

20. G.A. Somorjai and M.A. Van Hove, Progr. Surf. Sci. 30, 201 (1989).

21. R.J. Behm, D.K. Flynn, K.D. Jamison, G. Ertl and P.A. Thiel, Phys. Rev. B36, 9267 (1987).

22. M. Copel, W.R. Graham, T. Gustafsson and S. Yalisove, Sol. St. Commun. 54 695 (1985).

23. C.J. Barnes, M.Q. Ding, M. Lindroos, R.D. Diehl and D.A. King, Surf. Sci. 162, 59 (1985).

24. B.E. Hayden, K.C. Prince, P.J. Davie, G. Paolucci and A.M. Bradshaw, Sol. St. Commun. 48, 325 (1983).

25. R.J. Baird, D.F. Ogletree, M.A. Van Hove and G.A. Somorjai, Surf. Sci. 165, 345 (1986).

26. Y. Gauthier, in "Physics of Solid Surfaces 1987," Ed. J. Koukal, Elsevier (Amsterdam) 1988, p. 47.

27. D. Sondericker, F. Jona and P.M. Marcus, Phys. Rev. B33, 900 (1986).

28. B.E. Bent and G.A. Somorjai, J. Adv. Coll. Interf. Sci. 29, 223 (1989).

29. C.M. Mate, C.-T. Kao and G.A. Somorjai, Surf. Sci. 206, 145 (1988).

30. S.Y. Tong, H. Huang, C.M. Wei, W.F. Packard, F.K. Men, G.Glander and M.B. Webb, J. Vac. Sci. Technol. A6, 615 (1988).

31. J.B. Pendry, "Low-Energy Electron Diffraction: The Theory and its Application to Determination of Surface Structure," Academic Press (London) 1974.

32. L.J. Clarke, "Surface Crystallography: An Introduction to Low-Energy Electron Diffraction," Wiley-Interscience (Chichester) 1985.

33. J. Rundgren and A. Salwen, Comput. Phys. Commun. 9, 312 (1975).

34. W. Moritz and D. Wolf, Surf. Sci. 163, L655 (1985).

35. C.B. Duke and G.E. Laramore, Phys. Rev. B2, 4765 (1970); Phys. Rev. B2, 4783 (1970).

36. W. Moritz, H. Jagodzinski and D. Wolf, Surf. Sci. 77, 233 (1978); Surf. Sci. 77, 249 (1978).

37. J.B. Pendry, in "Determination of Surface Structure by LEED", P.M. Marcus and F. Jona, Eds., Plenum (New York) 1984.

38. J.B. Pendry and D.K. Saldin, Surf. Sci. 145, 33 (1984).

39. D.K. Saldin, D.D. Vvedensky and J.B. Pendry, in "The Structure of Surfaces", M.A. Van Hove and S.Y. Tong, Eds., Springer-Verlag (Berlin, Heidelberg, New York) 1985, p.131.

40. P.J. Rous and J.B. Pendry, Surf. Sci. 173, 1 (1986).

41. N. Masud and J.B. Pendry, J. Phys. C9, 1833 (1976).

42. F. Jona, J.A. Strozier, Jr. and P.M. Marcus, in "The Structure of Surfaces", M.A. Van Hove and S.Y. Tong, Eds., Springer-Verlag (Berlin, Heidelberg, New York) 1985, p.92.

43. M.A. Van Hove and G.A. Somorjai, Surf. Sci. 114, 171 (1982).

44. M.A. Van Hove, R.J. Koestner, J.C. Frost and G.A. Somorjai, Surf. Sci. 129, 482 (1983).

45. M.A. Van Hove, R. F. Lin and G.A. Somorjai, J. Am. Chem. Soc. 108, 2532 (1986).

46. M.A. Van Hove, R.F. Lin and G.A. Somorjai, Phys. Rev. Lett. 51, 778 (1983).

47. P.J. Rous, J.B. Pendry, K. Heinz, K. Mueller and N. Bickel, Phys. Rev. Lett. 57, 2951 (1986).

48. P.J. Rous, M.A. Van Hove and G.A. Somorjai, Surf. Sci. in press.

49. J.B. Pendry, K. Heinz and W. Ded, Phys. Rev. Lett. 61, 2853 (1988).

50. D.K. Saldin, J.B. Pendry, M.A. Van Hove, G.A. Somorjai, Phys. Rev. B31, 1216 (1985).

51. P.J. Rous, J.B. Pendry, D.K. Saldin, K. Heinz, K. Müller and N. Bickel, PHys. Rev. Lett. 57, 1951 (1986).

52. G.S. Blackman, M.-L. Xu, M.A. Van Hove and G.A. Somorjai, Phys. Rev. Lett. 61, 2352 (1988).

53. Z. P. Hu, D.F. Ogletree, M.A. Van Hove and G.A. Somorjai, Surf. Sci. 180, 433 (1987).

54. F. Jona and P.M. Marcus, in "The Structure of Surfaces II," Eds. J.F. van der Veen and M.A. Van Hove, Springer-Verlag (Heidelberg, Berlin) 1988, p. 90.

55. D.A. King, Physics World 2, 45 (1989).

56. K.A.R. Mitchell, S.A. Schlatter and R.N.S. Sodhi, Can. J. Chem. 64, 1435 (1986).

57. G.M. Lamble, R.S. Brooks, D.A. King and D. Norman, Phys. Rev. Lett. 61, 1112 (1988).

58. J. Onuferko, D.P. Woodruff and B.W. Holland, Surf. Sci. 87, 357 (1979).

59. W. Oed, H. Lindner, U. Starke, K. Heinz, K. Müller and J.B. Pendry, to be published.

60. W. Oed, H. Lindner, K. Heinz, K. Müller, D.K. Saldin, P. de Andres and J.B. Pendry, to be published.

61. H.D. Shih, F. Jona, D.W. Jepsen and P.M. Marcus, Phys. Rev. Lett. 46, 731 (1981).

62. D.G. Kelly, R.F. Lin, M.A. Van Hove and G.A. Somorjai, Surf. Sci. 204, 1 (1989).

63. H. Ohtani, M.A. Van Hove and G.A. Somorjai, in "The Structure of Surfaces II," Eds. J.F. van der Veen and M.A. Van Hove, Springer-Verlag (Heidelberg, Berlin) 1988, p. 219.

64. C.-T. Kao, G.S. Blackman, M.A. Van Hove, G.A. Somorjai and C.-M. Chan, Surf. Sci., in press.

65. D.J. Hannaman and M.A. Passler, Surf. Sci. 203, 449 (1988).

66. P. Hofmann, S.R. Bare, N.V. Richardson and D.A. King, Sol. St. Commun. 42, 645 (1982).

67. D.A. Wesner, F.P. Coenen and H.P. Bonzel, Surf. Sci. 199, L419 (1988).

68. M.R. Albert, J.T. Yates, Jr., "The Surface Scientist's Guide to Organometallic Chemistry," American Chemical Society (Washington, DC) 1987.

G.A. Somorjai and M.A. Van Hove, SURFACE CRYSTALLOGRAPHY BY LOW-ENERGY ELECTRON DIFFRACTION

LEGENDS

Figure 1.1 Schematic of a digital LEED system.

Figure 1.2. Example of a two-dimensional surface lattice (left) and its reciprocal lattice (right), which corresponds to the apots in the observed LEED pattern.

Figure 1.3. LEED patterns of a clean Pt(111) surface (left) and of the same surface with an ordered overlayer of acetylene (right). A spot at the center of the patterns and several other spots above the center are obstructed from view by the sample manipulator.

Figure 1.4. Real-space unit cells of the clean Pt(111)-(1x1) and Pt(111)-(2x2)-C_2H_2 surface structures.

Figure 1.5. Atomic arrangements in various unreconstructed, unrelaxed clean metal surfaces. In each panel, the top and bottom sketches give top and side views, respectively.

Figure 1.6. First-layer relaxation (negative is inward) plotted as a function of surface roughness (roughness = inverse of packing density). (After Jona and Marcus [54]).

Digital LEED Detector

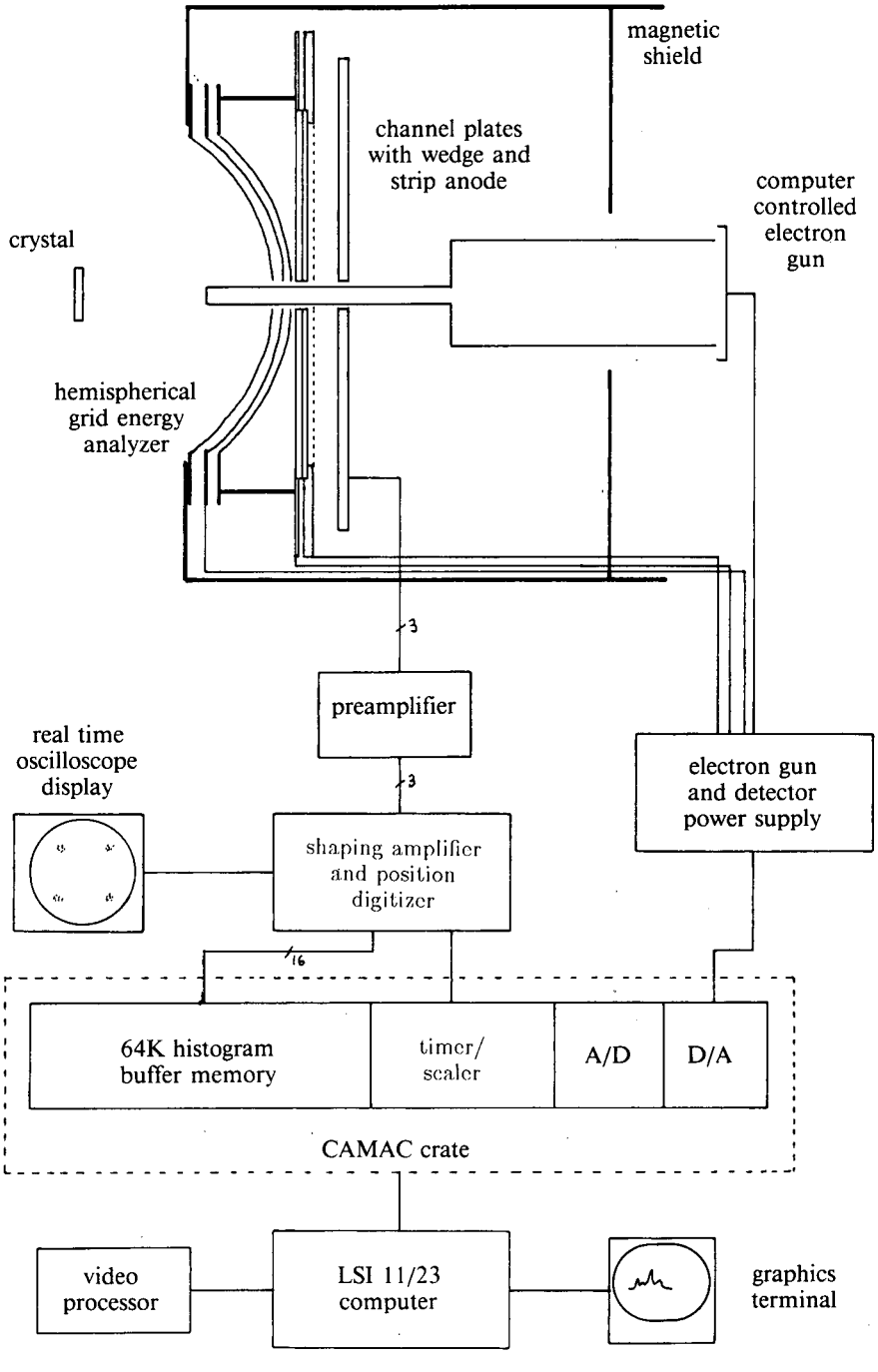

XBL 8512-5024

Fig. 1.1

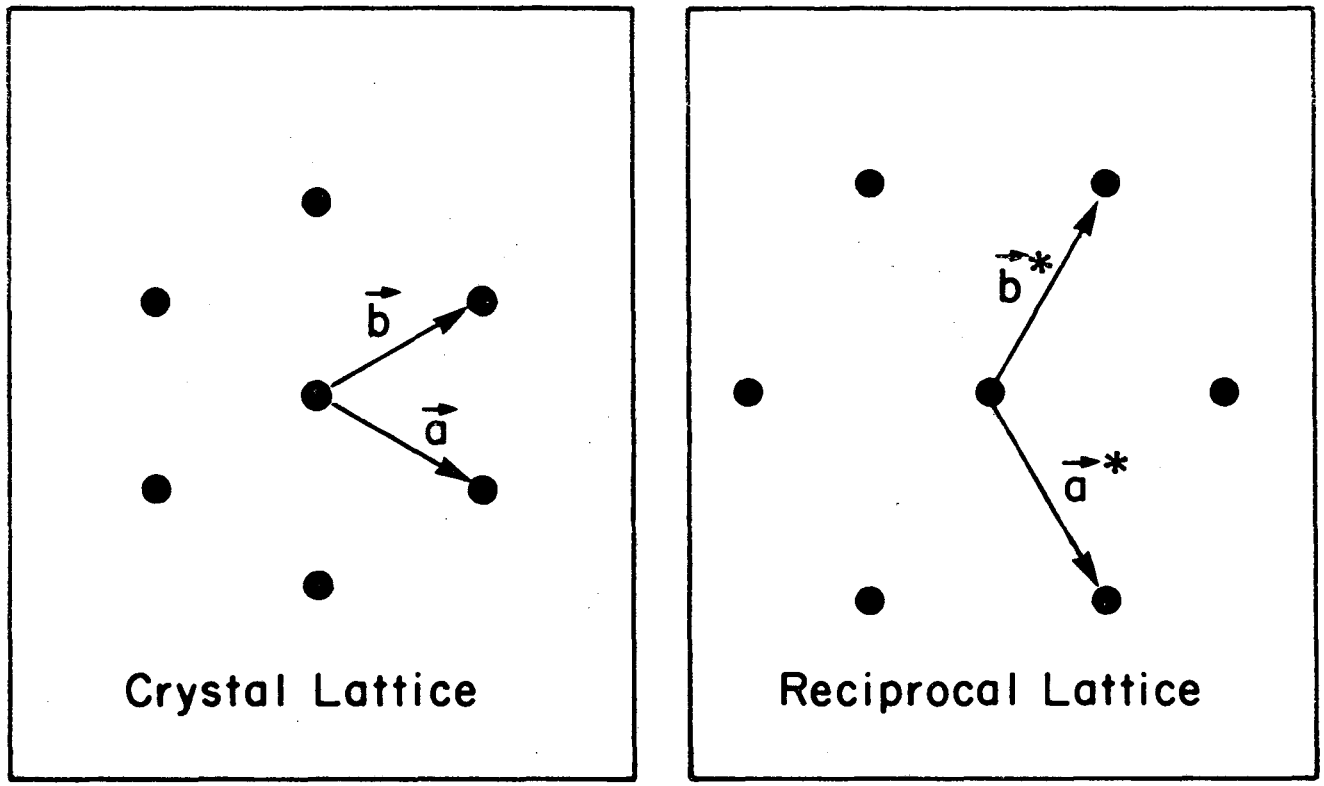

XBL 787-9590

Fig. 1.2

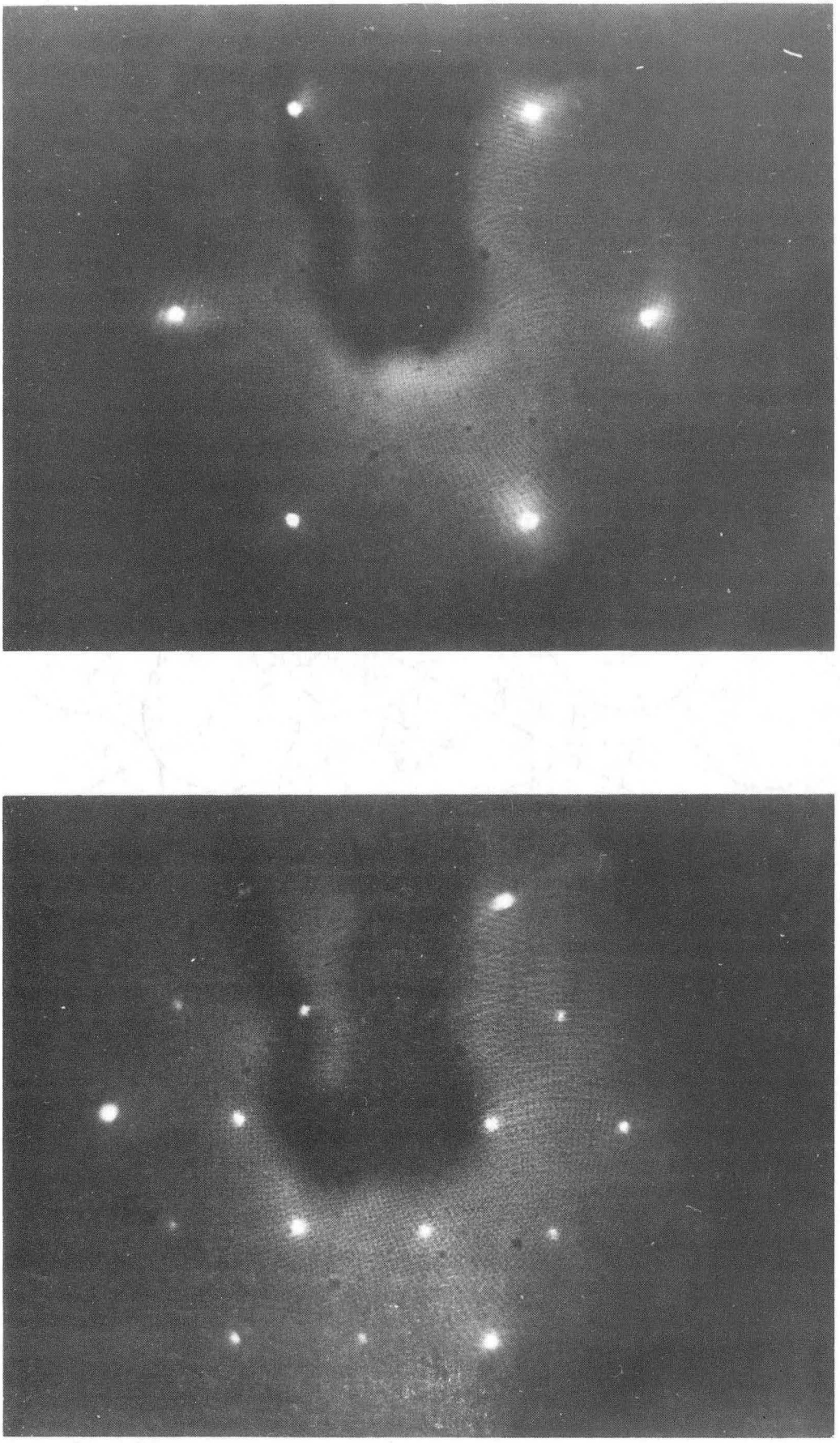

XBB750-8226

Fig. 1.3

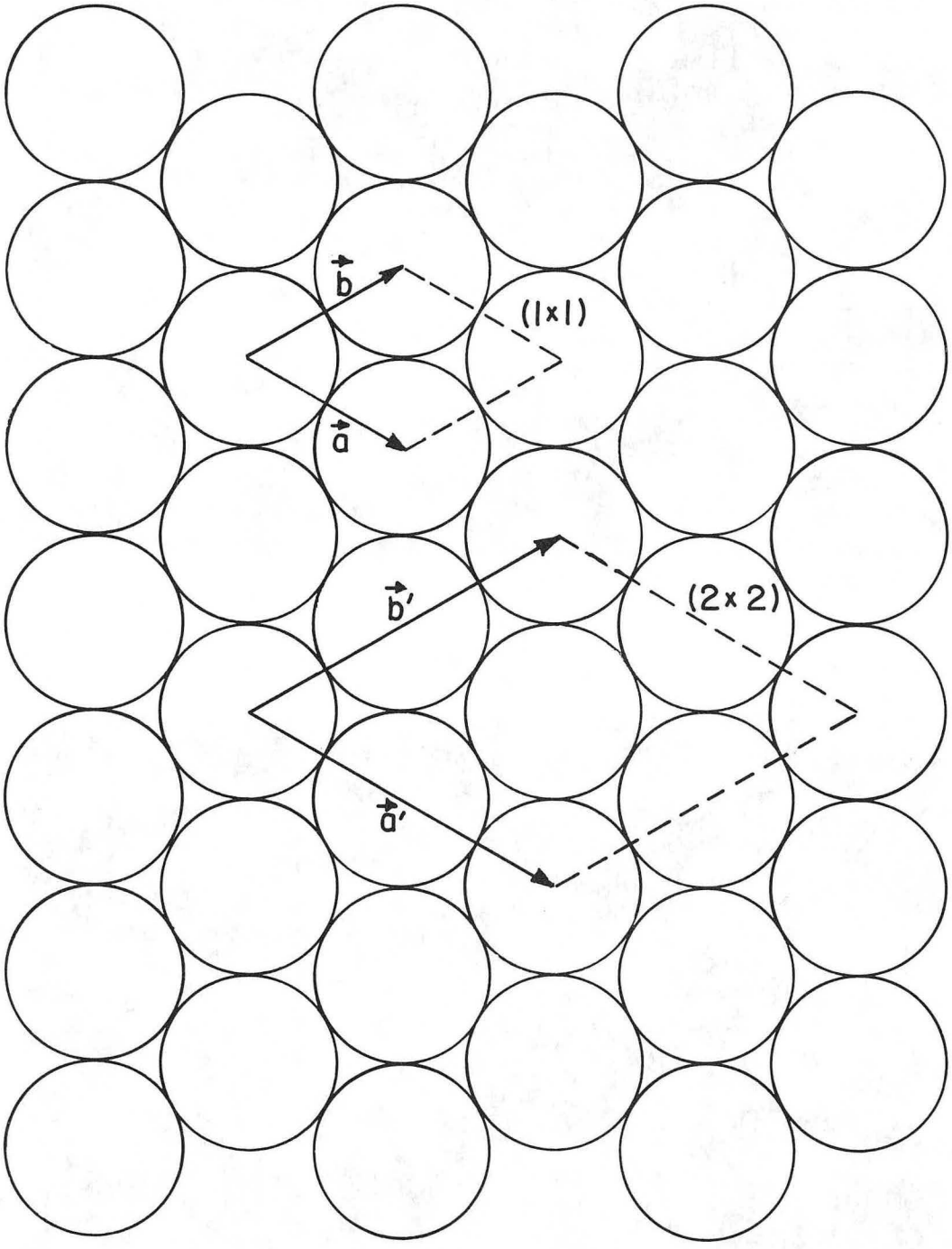

XBL7510-7551

Fig. 1.4

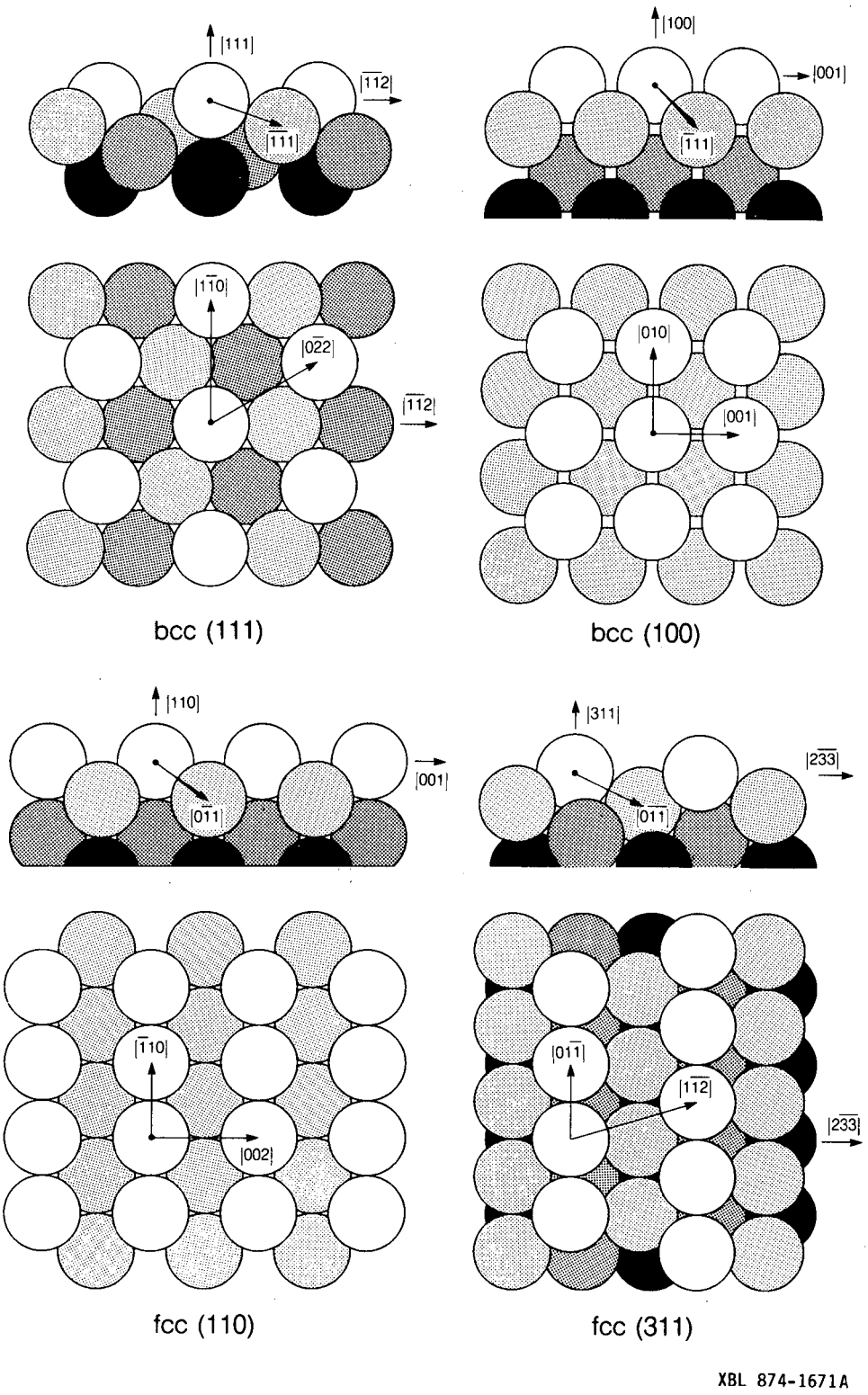
|111|
|11̄2|
|1̄11|
|100|
|001|
|1̄11|
|1̄10|
|02̄2|
|11̄2|
|010|
|001|
bcc (111)
bcc (100)
|110|
|001|
|01̄1|
|311|
|23̄3|
|01̄1|
|1̄10|
|002|
|01̄1|
|11̄2|
|23̄3|
fcc (110)
fcc (311)
XBL 874-1671A

Fig. 1.5

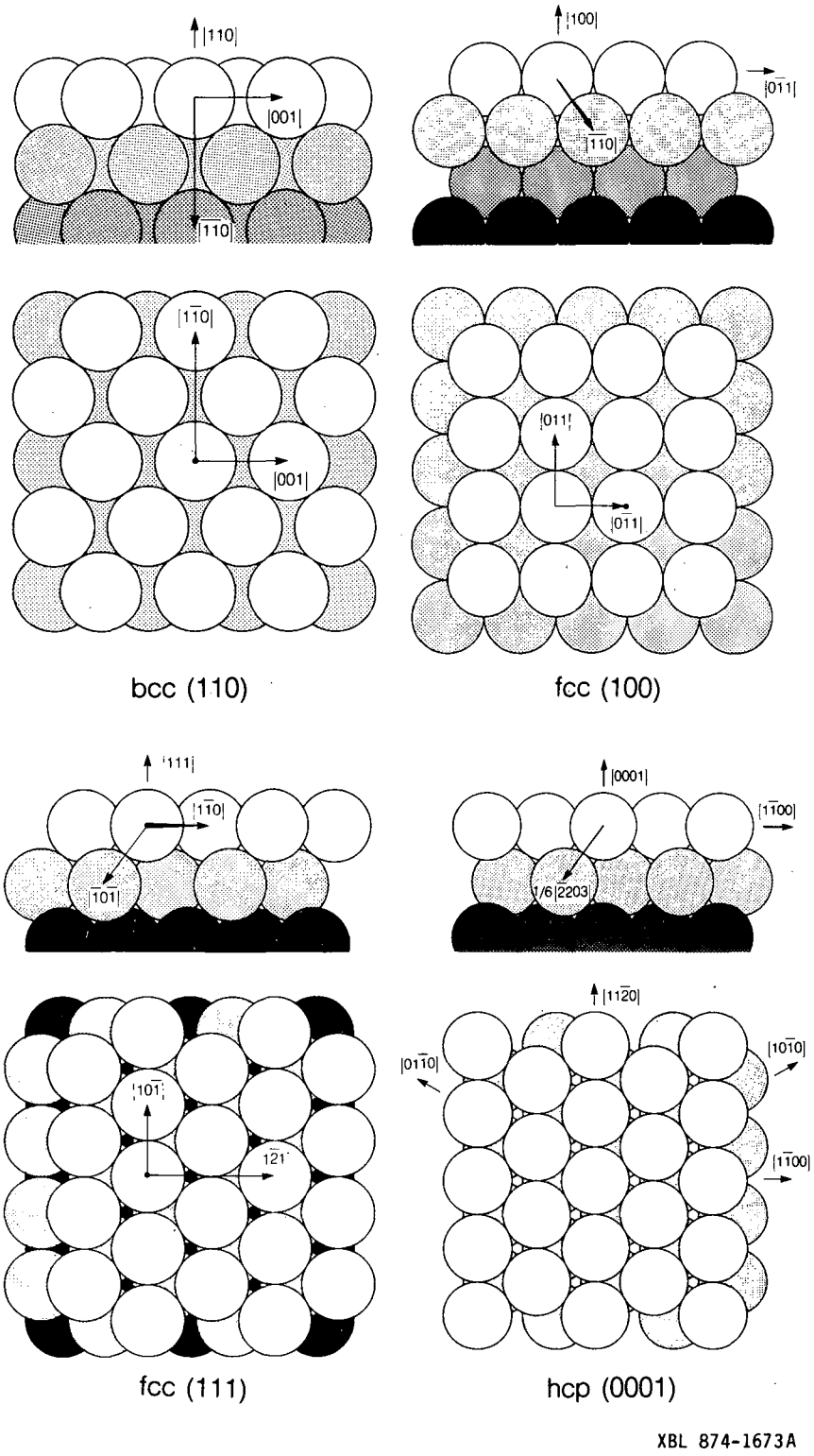
|110|
|001|
|1$\bar{1}$0|
|100|
|0$\bar{1}$1|
|110|
|1$\bar{1}$0|
|001|
|011|
|0$\bar{1}$1|
bcc (110)
fcc (100)
|111|
|1$\bar{1}$0|
|$\bar{1}$01|
|0001|
|1$\bar{1}$00|
1/6|2203|
|101|
1$\bar{2}$1
|11$\bar{2}$0|
|01$\bar{1}$0|
|10$\bar{1}$0|
|1$\bar{1}$00|
fcc (111)
hcp (0001)
XBL 874-1673A

Fig. 1.5

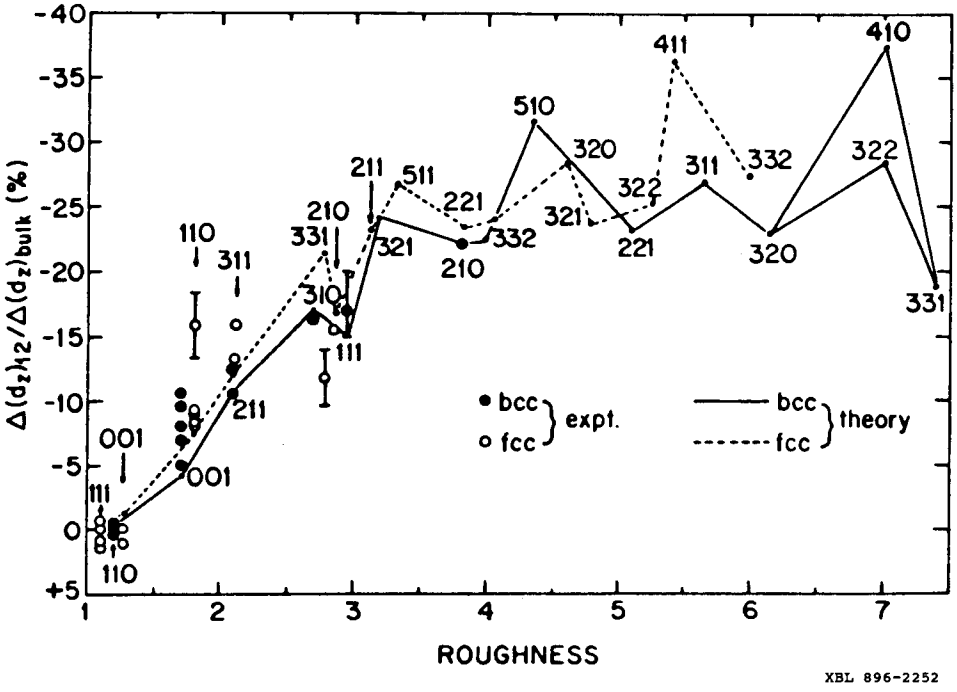

Experimental and theoretical first-layer relaxation (in %) as a function of roughness (=1/packing density) for several bcc and fcc surfaces.

Fig. 1.6

LAWRENCE BERKELEY LABORATORY
CENTER FOR ADVANCED MATERIALS
1 CYCLOTRON ROAD
BERKELEY, CALIFORNIA 94720